Technische Universität München
TUM School of Medicine and Health

Angiocrine HGF attenuates liver fibrosis by modulating the PDK1/Akt axis

Jianye Wang

Vollständiger Abdruck der von der TUM School of Medicine and Health der Technischen Universität München zur Erlangung des akademischen Grades eines

Doktors der Medizin (Dr.med.)

genehmigten Dissertation.

Vorsitz: Prof. Dr. Susanne Kossatz

Prüfende der Dissertation:

1. apl. Prof. Dr. Norbert Hans Hüser
2. apl. Prof. Dr. Guido von Figura

Die Dissertation wurde am 20.07.2023 bei der Technischen Universität München eingereicht und durch die TUM School of Medicine and Health am 20.12.2023 angenommen.

TABLE OF CONTENTS

ABBREVIATIONS

CCl_4	Carbon tetrachloride
HCC	Hepatocellular carcinoma
DAPI	4', 6-diamidino-2-phenylindole
ECM	Extracellular matrix
HRP	Horseradish peroxidase
IHC	Immunohistochemistry
NC	Non-specific control
PBS	Phosphate buffered solution
qRT-PCR	Quantity real-time polymerase chain reaction
H&E	Hematoxylin and Eosin
WB	Western blot
HGF	Hepatocyte growth factor
LSEC	Liver sinusoidal endothelial cell
EC	Endothelial cell
HSC	Hepatic stellate cell
ALT	Alanine transaminase
DNA	Deoxyribonucleic acid
RNA	Ribonucleic acid
IF	Immunofluorescence
TGF-β	Transforming growth factor beta
AQP4	Aquaporin-4
RNA-seq	RNA sequencing
Stab2	Stabilin 2
WT	Wild type
Tg	Transgene
COL1A1	Collagen type I alpha chain 1
α-SMA	Alpha smooth muscle actin
GBSS	Gey´s Balanced Salt Solution
HBSS	Hank's Balanced Salt Solution

TBS	Tris Buffered Saline
VEGF	Vascular endothelial growth factor
SPF	Specific pathogen free
MRI	Magnetic resonance imaging
SDS	Sodium Dodecyl Sulfate
SDS-PAGE	SDS- polyacrylamide gelelectrophoresis
PI	Protease Inhibitor
TGF-β1	Transforming growth factor β1
ECM	Extracellular matrix
KC	Kupffer cell

LIST OF TABLES

LIST OF FIGURES

ABSTRACT

INTRODUCTION

Hepatocyte growth factor (HGF) is a complete hepatic mitogen and is believed to play a role in liver fibrogenesis. Liver sinusoidal endothelial cells (LSEC) can recruit inflammatory cells by releasing angiocrine signals in the process of liver fibrogenesis, but the precise contributions of HGF from LSEC to hepatic fibrosis remains unelucidated.

METHODS

To investigate the effects of hepatic angiocrine HGF on liver fibrogenesis, Stab2-Cre^{tg} HGF$^{fl/fl}$ (HGF$^{LSEC-KO}$) mice, in which HGF is specifically switched off in LSEC, were used. Carbon tetrachloride (CCl_4) injection was performed in these mice and the kinetics of the liver to body weight ratio, immunohistochemistry for liver fibrosis, Western blot and RT-PCR for fibrotic markers, HGF/c-MET related pathways, and cell cycle-associated genes were determined after initiation of fibrosis.

RESULTS

We found that HGF$^{LSEC-KO}$ mice showed no difference in the relative liver weight alteration after early-stage CCl_4 treatment. HGF$^{LSEC-KO}$ mice exhibited a higher expression of collagen 1A1 and alpha-SMA and the proliferation of hepatocytes was significantly impaired in HGF$^{LSEC-KO}$ mice. In addition, the LSEC-specific HGF deficiency reduced the c-met level and thus deactivated the PDK1 (3-phosphoinositide-dependent protein kinase-1)/Akt pathway while hepatic angiocrine HGF did not alter immune cell infiltration. Noteworthy, Aquaporin-4 (AQP4) is strongly expressed in the setting of HGF deficiency in LSEC.

CONCLUSIONS

The hepatic angiocrine HGF signalling pathway plays a crucial role in the early stages of liver fibrogenesis, and the PDK1/Akt axis are mostly influenced by the deletion of LSEC-specific HGF.

1 INTRODUCTION

1.1 Pathogenesis of liver fibrosis

Liver fibrosis is a repair response after liver injury, characterised by excessive deposition of extracellular matrix (ECM), which results from abnormal ECM increase and decreased matrix degradation (Aydin and Akcali 2018). Hepatic fibrosis is mainly related to persistent liver injury, inflammatory response, and activation of hepatic stellate cells (HSCs) (Friedman 2003; Parola and Pinzani 2019). There are many factors can induce liver injury, such as viral or parasitic infections, biliary stasis, metabolic diseases, nutrition, parasite, genetics, and long-term excessive alcohol intake. The pathophysiological mechanisms of liver fibrosis are complex, which consist of a variety of cellular and cytokine factors. Usually, hepatocytes in the liver in response to injury factors can trigger the release of a series of cellular contents and cytokines, among which the injury-associated molecular pattern activates blast cells to produce inflammatory cytokines, which in turn activate HSCs (Figure 1) (Bao, Wang et al. 2021; Zhangdi, Su et al. 2019). Among them, quiescent hepatic stellate cells (qHSCs) are activated into myo-fibroblast-like cells (MFBLCs) that produce a large quantity of ECM, named as activated hepatic stellate cells (aHSCs). aHSCs are central events in the formation and development of liver fibrosis (Hernandez-Gea and Friedman 2011). Studies have revealed that the occurrence and development of liver fibrosis is a dynamic process, including multiple cells (such as HSCs, hepatic sinusoidal endothelial cells, macrophages), multiple molecules (such as NF-κB, TGF-β1, TNF), and multiple signalling pathways (such as NF-κB, TGF-β1/Smad, PI3K/Akt, Hedgehog, Wnt/β-catenin) (Bataller and Brenner 2005). Even though considerable studies have shown that liver fibrosis is reversible (Campana and Iredale 2017; Ebrahimi, Naderian et al. 2018;

Zoubek, Trautwein et al. 2017), as a common pathological stage of chronic liver disease, persistent liver fibrosis can further progress to cirrhosis, liver failure, or hepatocellular carcinoma, ultimately leading to the death of the patient (Duspara, Bojanic et al. 2021).

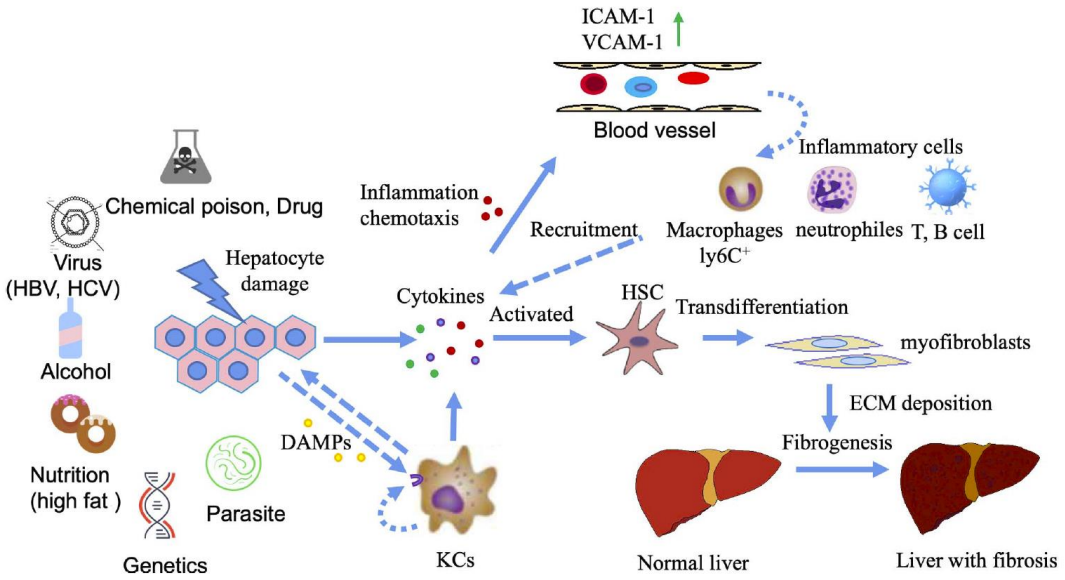

Figure 1. Pathogenesis of hepatic fibrosis
Liver injury can be caused by a diversity of factors, including viruses, drugs, nutrition, parasites, genetics, and others. The injured liver cells can produce DAMPs that stimulate Kupffer cells to release inflammatory cytokines. In the injured sites, the permeability of blood vessel increases. With the cytokines, it exhibited high recruit capability for inflammatory cells. HSCs were next activated by the cytokines and can produce the ECM. The persistent injury and inflammation can lead to the ECM deposition and liver fibrosis (Bao, Wang et al. 2021).

1.2 HSC activation in liver fibrosis

HSCs, also known as vitamin A storage cells, fat storing cells, and Ito cells, are a kind of interstitial cell of the liver, located in the Disse cavity between hepatocytes and hepatic sinusoidal endothelial cells, accounting for 5%–8% of all liver cells (Sufletel, Melincovici et al. 2020). Activation of HSCs is now recognised as a key event in the progression of liver fibrosis (Zhangdi, Su et al. 2019). aHSCs further promote the production of pro-inflammatory and pro-fibrotic factors, activate qHSCs step by step, and activate signalling pathways such as NF-κB, and positive feedback regulates the

formation of liver fibrosis (Higashi, Friedman et al. 2017). Normally, HSCs exist in a non-dividing quiescent form and have various physiological functions (Friedman 2008; Geerts 2001; Senoo, Yoshikawa et al. 2010; Yin, Evason et al. 2013), such as (1) uptake, storage, and release of vitamin A, and storage of lipid droplets; (2) release of matrix metalloproteinases (MMPs, such as MMP2, MMP3, MMP10, MMP13, MMP14) and their inhibitors by secreting an appropriate amount of ECM molecules (mainly collagen type III, collagen IV, laminin)—tissue inhibitors of metalloproteinases (TIMPs, such as TIMP1, TIMP2) involved in the formation, remodelling, and degradation of ECM; (3) regulation of hepatic sinusoidal blood flow (Geerts 2001); (4) secretion of a variety of cytokines (Friedman 2008) and participation in liver regeneration (Yin, Evason et al. 2013) and immune regulation. When the liver is stimulated by damage, under the activation of paracrine and autocrine signals, HSCs are activated and transformed into aHSCs (Tsuchida and Friedman 2017). This activation process mainly includes two stages: “initiation” and “perpetuation”. During the “initiation” phase, the injured liver is more responsive to cytokines and other local stimuli, and factors such as paracrine stimuli from various adjacent cell populations and changes in ECM composition greatly stimulate HSC activation (Puche, Saiman et al. 2013). As to the “perpetuation” stage, the stimulation from autocrine, paracrine, and the acceleration of ECM remodelling continuously activates HSCs. Subsequentially, the structure and function of HSCs greatly change (Puche, Saiman et al. 2013; Schuppan and Popov 2002), manifesting mainly in (1) a mass decrease or disappearance of lipid droplets and vitamin A in the cytoplasm, (2) high expression of α-smooth muscle actin (α-SMA, HSCs activation marker), vimentin, and desmin, (3) an increase in the secretion of ECM, producing a large amount of ECM proteins (such as collagen type I, collagen type III, laminin, sulphated proteoglycans, glycoproteins), (4) acquired contractile properties, increased proliferation ability and fibre formation ability, and enhanced chemotaxis, and (5) the

increased synthesis and secretion of TIMPs and inhibited activity of MMPs, resulting in massive deposition of ECM (Tsuchida and Friedman 2017). This series of changes eventually leads to massive deposition of ECM and the formation of liver fibrosis.

1.3 The role of LSECs in liver fibrosis

Liver sinusoidal endothelial cells (LSECs) are single-layer and flattened endothelial cells that line the hepatic sinusoids. This particular structure was first proposed in 1970 (Wisse 1970). As a special type of vascular endothelial cells, LSEC has many fenestrations without septa, the cell membrane is sieve-like, and there is no intact subendothelial basement membrane. The intercellular junctions of LSEC are loose and mainly composed of typical endothelial cell adhesion proteins (such as VE-cadherin, (α-/β-)p120-catenin, and plakoglobin) and atypical endothelial cell tight junction proteins (such as JAM-A, JAM-B, JAM-C, and zonula occludens proteins ZO-1 and ZO-2) (Geraud, Evdokimov et al. 2012).

The highly permeable structure of LSEC greatly promotes the material exchange between hepatic sinusoidal blood and hepatocytes, selectively filters substances of different molecular sizes, and is essential for the maintenance of hepatic sinusoidal homeostasis. In liver fibrosis, the LSEC fenestration disappears and an intact subendothelial basement membrane forms, a phenomenon known as “LSECs capillarisation” (Xing, Zhao et al. 2016). Concurrently, HSCs are activated to become myofibroblasts, secrete a large amount of ECM, increase the tension of hepatic sinusoids, and dissolve the microvilli of hepatocytes (Poisson, Lemoinne et al. 2017). In patients at any degree of chronic active hepatitis, or in laboratory liver fibrotic models, the capillarisation of LSECs precedes the occurrence of hepatic fibrosis (Bardadin and Desmet 1985; DeLeve, Wang et al. 2008b; Pasarin, La Mura et al. 2012). This provides

a clue that the capillary vascularisation of hepatic sinusoidal endothelial cells may trigger liver fibrosis.

The normal differentiation state of hepatic sinusoidal endothelial cells is important for the homeostasis of hepatic sinusoids. Co-culture of fenestrated state LSECs and HSCs can maintain the quiescent state of HSCs, while capillarised LSECs promote HSC activation and differentiated LSECs can reverse the activation state of HSCs (DeLeve, Wang et al. 2008b; Xie, Wang et al. 2012). Besides, the maintenance of the normal differentiation state of LSEC mainly depends on vascular endothelial growth factor (VEGF). Hepatocyte and HSC-derived VEGF maintains the fenestrated state of LSEC through endothelial nitric oxide synthase (eNOS)—mediated NO-independent pathway (May, Djonov et al. 2011; Xie, Wang et al. 2012). Based on the study of Hedgehog signalling pathway inhibitors and Hedgehog ligand neutralising antibodies, it is revealed that Hedgehog signalling induces capillary vascularisation in LSECs (Chapouly, Guimbal et al. 2019). In mice with specific smoothened gene knockout, inhibiting the activation of the Hedgehog signalling pathway can reduce the expression of LSEC capillary-related genes (Xie, Choi et al. 2013). Another study showed that liver X receptors (LXRs) can inhibit Hedgehog signalling, thereby suppressing the capillary vascularisation of LSECs (Xing, Zhao et al. 2016). Some studies have shown that statins can improve portal hypertension caused by liver fibrosis in rats, mainly by inducing the expression of eNOS and the phosphorylation of eNOS, which has a protective effect on LSECs (Abraldes, Rodriguez-Vilarrupla et al. 2007). Additionally, statins can also promote the high expression of Kruppel-like transcription factors (KLF)-2 in HSCs. Researchers proposed the role of the lipid rafts-cribriform hypothesis in the formation and regulation of the fenestration of LSECs. Lipid rafts are regions of the cell membrane that are rich in sphingolipids and cholesterol responsible for membrane stabilisation, provide binding platforms for various cell membrane

proteins (such as caveolin), and anchor the cytoskeletal actin protein to maintain stabilisation and integrity. When the role of actin and lipid rafts in stabilising the cell membrane is weakened, the non-lipid raft region on the LSEC membrane begins to form a fenestrated structure (Cogger, Roessner et al. 2013; Svistounov, Warren et al. 2012). Many factors such as inflammation, excessive dietary fat, vasoactive cytokines, and hormones, including those factors that can affect the actin cytoskeleton, such as cytochalasin D, latrunculin A, calcium ion concentration, VEGF, and the Rho-like GTPases protein family, can affect the number and size of LSEC fenestrations (Cogger, Roessner et al. 2013). Subendothelial basement membrane formation is another major feature of LSEC capillarisation. Studies have shown that collagen type IV, laminin, fibronectin, and other cell basement membrane components participated in patients with alcoholic liver disease and chronic active hepatitis or CCl_4-induced rat liver fibrosis model. The expression of the above constituents in the mid-sinusoidal space was significantly increased (Hahn, Wick et al. 1980; Nakayama, Takahara et al. 1993). Co-localisation of collagen type IV with laminin may suggest the formation of the basement membrane of hepatic sinusoidal endothelial cells during liver fibrosis (Mak, Chen et al. 2013). The expression of type I, III, and IV collagen and laminin mRNA can be detected in normal rat LSECs, while the expression increased in CCl_4-induced liver fibrosis (Maher and McGuire 1990).

Furthermore, the 35S probe for laminin Bl detection demonstrated that normal human liver bile duct epithelial cells, portal interstitial cells, and LSECs can express laminin protein. The expression of laminin in the liver tissue of patients with liver fibrosis or cirrhosis is significantly increased (Milani, Herbst et al. 1989). Perlecan, an important heparan sulphate proteoglycan secreted by LSEC, can bind to cell basement membrane components (Rescan, Loréal et al. 1993). When the liver is damaged, LSEC can secrete fibronectin isoform EIIIA (fibronectin EDA), which can promote the differentiation of

HSC into myofibroblasts (Jarnagin, Rockey et al. 1994). In the process of liver fibrosis, capillary LSEC secretes transforming growth factor-beta (TGF-β), which can directly activate HSC, and TGF-β can promote LSEC to secrete fibronectin alternative splicing of extra domain A (EIIIA) to further activate HSC (George, Wang et al. 2000). These studies indicate that the increased secretion of basement membrane proteins by endothelial cells during capillarisation of LESCs is the main reason for the formation of subendothelial basement membranes.

In addition to synthesising cell basement membrane and extracellular components, LSECs are essential in the deposition of ECM in the Disse space and the metabolism degradation of ECM. Some studies have found that NO derived from vascular endothelial cells can reduce the content of type I and III collagen in vascular smooth muscle cells (Myers and Tanner 1998). The differentiation of HSCs into myofibroblasts requires not only ECM, but also ECM-mediated mechanical tension and adhesion to matrix proteins (Olsen, Bloomer et al. 2011). With the increase of matrix hardness, there is more activation of primary HSCs. When HSCs were implanted in high-hardness and high-elasticity polytetrafluoroethylene polymer materials, HSCs were not activated due to the inability to conduct mechanical tension. RhoA regulates cytoskeleton organisation and cell migration through non-receptor tyrosine protein kinase (c-SRC) in a variety of cells. As the ECM deposits, the expression of RhoA in HSCs increases accompanied by inhibiting c-SRC and promoting its transformation into myofibroblasts, which promotes the progression of liver fibrosis (Liu, You et al. 2017).

The communication between LSEC and other liver cells is another vital factor in the development of liver fibrosis (Marrone, Shah et al. 2016). In the process of chronic liver injury, hepatocytes damaged are always accompanied by capillary vascularisation of LSECs, hepatocyte necrosis, HSC and Kupffer cell (KC) activation, and inflammatory

cell infiltration (Aydin and Akcali 2018). Among them, the expression of fibroblast growth factor receptor 1 (FGFR1) in LSECs increases, which leads to the expression of chemokine receptor 4 (CXCR4) and CXCR7 in LSECs. The increased ratio eventually leads to the transformation of the microenvironment of liver regeneration mediated by CXCR7 of LSECs to the microenvironment of hepatic fibrosis mediated by CXCR4 (Ding, Cao et al. 2014). As a transmembrane glycoprotein, CD147 is also a key factor in the progression of liver fibrosis. The expression of CD147 in LSECs was significantly increased in patients with hepatitis B virus (HBV)-related hepatic fibrosis (Zhang, Zhao et al. 2012). CD147 can induce the secretion of VEGF-A in hepatocytes through the PI3K/Akt pathway, and simultaneously promote the expression of VEGFR2 in LSECs and promote angiogenesis during liver fibrosis (Yan, Qu et al. 2015). The application of CD147 antibody could inhibit VEGF-A/VEGFR-2-mediated hepatic angiogenesis and thus alleviate liver fibrosis. In addition, HSCs and bile duct epithelial cells can secrete Hedgehog ligand-rich exosomes during liver fibrosis to promote capillary vascularisation of LSECs (Witek, Yang et al. 2009). LSEC-derived sphingosine kinase 1 (SK1)-rich exosomes can promote HSC activation (Wang, Ding et al. 2015). Programmed cell death-1 (PD-1)-positive Kupffer cells lead to sepsis-induced LSEC injury by binding to PD-L1 of the surface of LSECs (Hutchins, Wang et al. 2013). Moreover, in septic liver injury, Kupffer cells secrete considerable interleukin-1 (IL-1) and tumour necrosis factor-α (TNFα), which mediate the expression of Molecules-1 (intracellular adhesion molecule-1, ICAM-1) in LSECs. Whereas ICAM-1 promotes leukocyte adhesion to LSEC (Arii and Imamura 2000).

Angiogenesis during liver fibrosis induces collagen fibre remodelling, wherein collagen fibres are more tightly cross-linked and denser. Vascular remodelling during liver fibrosis has increasingly been spotlighted in fibrosis research since pathological angiogenesis is closely related to liver fibrosis, and it can promote the development of

liver fibrosis, and eventually progresses to liver cirrhosis or liver cancer. Vascular remodelling during liver fibrosis mainly includes capillary vascularisation of LSECs and formation of a portal-systemic shunt (Zhao, Amevor et al. 2023). Taking the formation of chronic liver cirrhosis as an example, after fibrosis develops to a certain degree, it's always accompanied by the remodelling of vasculature. The fibrous septum connects the portal area and the central venous area, where the new vascularised fibrous septum communicates directly between the portal tracts and central veins (Schuppan and Afdhal 2008). The blood that normally flows through the hepatic sinusoids and hepatocytes for nutrient exchange will bypass the lobules and flow directly into the central vein via these new blood vessels. The hepatic lobules without blood supply will die out successively and eventually lead to liver cirrhosis or liver failure (Ma, Reiter et al. 2020).

Inflammation and hypoxia are additional key factors promoting pathological angiogenesis during liver fibrosis. With persistent liver injury, immune cells in the blood of liver sinusoids are rapidly recruited to the damaged site to resist damage and remove necrotic substances (Fernandez, Semela et al. 2009). Persistent liver injury and inflammatory response lead to increased hepatic vascular permeability and enhances chemokine-mediated recruitment of inflammatory cells. Inflammatory cells secrete many angiogenic factors and growth factors to promote the proliferation and migration of vascular endothelial cells. In addition, chronic inflammation and deposition of fibrous tissue leads to a hypoxic environment in liver tissue. The increased production of hypoxia-inducible factors (HIFs) further promotes hepatocytes and HSCs to secrete a profusion of VEGFs, PDGFs and other factors that promote angiogenesis (Cannito, Paternostro et al. 2014; Paternostro, David et al. 2010). In animal models of liver fibrosis induced by bile duct ligation, CCl_4 and high-fat feeding, the expression of VEGF was significantly increased in the hypoxic area of liver tissue (Moon, Welch et al.

2009).

1.4 The role of HGF in liver disease

The A chain contains four Kringle domains, and there is a hairpin-like structure at the N-terminus of the A chain. The pro-HGF, an inactivated precursor, is a single polypeptide that is bound to hepatic ECM (Mohammed, Pennington et al. 2005). As the processing of ECM remodelling, the ECM-bound HGF releases the store of growth factors (Lamszus, Joseph et al. 1996; Liu, Mars et al. 1994; Masumoto and Yamamoto 1991). An *in vitro* proliferation experiment shows the single-chain HGF is inactive in hepatocytes in the presence of serine protease inhibitors, whereas the two-chain form of HGF is activated via proteolytic cleavage, creating a two-chain peptide (Miyazawa 2010). HGF was discovered as a substance that can stimulate the proliferation of hepatocytes, which acts on hepatocytes and can promote the growth and regeneration of hepatocytes (Yu, Chen et al. 2021). Given liver is the metabolic centre of the body, and studies have confirmed that HGF can affect liver metabolism. Besides, HGF is an evolutionarily conserved multifunctional protein, and studies over the past decade have confirmed that it is involved in cellular stress, proliferation, cycle regulation, DNA damage repair, transcription and post-transcriptional regulation, and other biological events (Tatsumi 2010). HGF mainly comes from liver Kupffer cells, endothelial cells, fibroblasts, fat storage cells, lung endothelial cells, and malignant tumour cells. Many studies have shown that HGF is the strongest mitogen of hepatocytes. It originally exists in the form of an inactive single-chain, and next acts on c-Met to form the HGF/c-Met signal transduction system after being converted into an active heterodimer (De Silva, Roy et al. 2017). After binding to HGF, c-Met can affect transcription in the nucleus by activating the receptor tyrosine kinase pathway, thereby affecting cell proliferation, differentiation, and apoptosis, and playing an important role in the regeneration of

hepatocytes (Zhao, Ye et al. 2022). Besides, HGF has been shown to participate in liver regeneration and initiating liver regeneration after liver injury and alleviating liver fibrosis (Seo, Sohn et al. 2014). However, the specific role of HGF located in LSECs in liver fibrogenesis has not yet been discussed. In the current study, we focused on the crosstalk between LSEC and HSC in the hepatic vascular niche and the specific regulatory mechanism of HGF affecting HSC activation, which is essential for scrutinising the therapeutic methods in liver fibrogenesis.

2 AIMS OF THIS STUDY

HGF belongs to the Kringle protein family with a three-leaf dimer ring structure. HGF originally exists in the body in the form of an inactive single-chain, after being cleaved by various proteases, it can be converted into an active heterodimer that acts on c-Met to form the HGF/c-Met signal transduction system. HGF is a potent mitogen for hepatocytes and has the function of initiating liver regeneration after liver injury. Nevertheless, the LSEC-specific contribution of HGF in liver fibrogenesis is not well elucidated.

The aims of the study are from the following aspects:

1. To determine whether there is a difference of HGF protein expression in normal and fibrotic human LSECs and what the relationship is between LSEC-specific HGF and fibrotic level.

2. Consider whether LSEC-specific knockout impacts liver fibrosis in a mouse model and in which period the most significant impact is exhibited.

3. To investigate which molecular mechanisms are influenced by the deletion of LSEC-specific HGF during liver fibrosis.

4. To evaluate whether a HGF LSEC-specific knockout contributes to fibrogenesis and the function of HGF in LESCs in it.

3 MATERIALS AND METHODS

3.1 Materials

3.1.1 Chemicals and reagents

Table 1: Chemicals and reagents

Name	Source
2-Mercaptoethanol C_2H_6OS	Sigma-Aldrich, Germany
4′, 6-Diamidino-2-phenylindole (DAPI)	Sigma-Aldrich, Germany
Acetic acid ($C_2H_4O_2$)	AppliChem, Germany
Agarose	Sigma-Aldrich, Germany
Albumin from bovine serum (BSA)	Sigma-Aldrich, Germany
Ammonium Persulphate (APS)	Sigma-Aldrich, Germany
Bromphenol blue	Sigma-Aldrich, Germany
Calcium chloride ($CaCl_2$)	Sigma-Aldrich, Germany
D (+) - Glucose $C_6H_{12}O_6$	Sigma-Aldrich, Germany
DAB System	Dako, USA
Deoxynucleotide (dNTP) solution mix	New England Biolabs, Germany
Dimethyl sulphoxide (DMSO) C_2H_6OS	Sigma-Aldrich, Germany
DirectPCR Lysis Reagent Tail	PEQLAB, Germany
dNTP Set (10 mM)	ThermoFisher, USA
Dulbecco's phosphate buffered saline (dPBS)	Sigma-Aldrich, Germany
ECL detection reagent	Amersham, USA
Ethanol (EtOH) 50%, 70%, 96%, 100%	Carl Roth, Germany
Ethidium bromide (EB)	Carl Roth, Germany
Ethylene diamine tetra-acetic acid (EDTA)	Sigma-Aldrich, Germany
Fetal Bovine Serum Superior (FCS)	Biochrom, Germany
Gel loading dye, purple (5×)	ThermoFisher, USA
Glacial acetic acid	Sigma-Aldrich, Germany

Glucose ($C_6H_{12}O_6$)	Sigma-Aldrich, Germany
Glutamine	Invitrogen GmbH, Germany
Glycerol ($C_3H_8O_3$)	AppliChem, Germany
Glycine ($C_2H_5NO_2$)	Carl Roth, Germany
Haematoxylin	Merck, Germany
Heparin sodium salt	Sigma-Aldrich, Germany
HEPES (4-(2-hydroxyethyl)-1-piperazine-ethanesulfonic acid))	Sigma-Aldrich, Germany
HEPES buffer	Sigma-Aldrich, Germany
Hydrochloric acid HCl	Carl Roth, Germany
Hydrogen Peroxide (30%)	Carl Roth, Germany
Magnesium chloride ($MgCl_2$)	Carl Roth, Germany
Magnesium sulphate ($MgSO_4$)	Sigma Aldrich, Germany
Medium DMEM (1×)	Gibco, USA
Methanol (CH_3OH)	Sigma-Aldrich, Germany
$MgSO_4$	Sigma-Aldrich, Germany
Milk Powder (Blotting-Grade)	Carl Roth, Germany
N, N, N′, N′ - Tetramethylethylenediamine (TEMED)	Biorad Laboratories, Germany
Oligo (dT)18 Primer	ThermoFisher, USA
Olive oil	Sigma-Aldrich, Germany
Paraformaldehyde (PFA)	Sigma-Aldrich, Germany
Penicillin/Streptomycin (Pen/Strep)	Biochrom, Germany
Permanent Mounting Medium	Vector laboratories, USA
Peroxidase Suppressor	ThermoFisher, USA
Potassium chloride (KCl)	Carl Roth, Germany
Potassium-bicarbonate ($KHCO_3$)	Sigma-Aldrich, Germany
Propanolol (C_3H_8O)	Sigma-Aldrich, Germany
Recombinant Human HGF	R&D Systems, USA
Recombinant Mouse HGF	R&D Systems, USA
RiboLock RNase Inhibitor	ThermoFisher, USA
RNA free water	ThermoFisher, USA

Roticlear	Carl Roth, Germany
Sirius Red Solution	Sigma-Aldrich, Germany
Sodium acetate ($C_2H_3NaO_2$)	AppliChem, Germany
Sodium bicarbonate ($NaHCO_3$)	Sigma-Aldrich, Germany
Sodium chloride (NaCl)	Sigma-Aldrich, Germany
Sodium dodecyl sulphate (SDS) Pellets	Carl Roth, Germany
Sodium hydroxide (NaOH)	Sigma-Aldrich, Germany
Sodium phosphate dibasic (Na_2HPO_4)	Sigma-Aldrich, Germany
ß-Mercaptoethanol	Merck, Germany
SYBR Green 1 Master Kit	Roche, Germany
Tris (Triphenylphosphine) rhodium (I) chloride (Tris-Cl)	Sigma-Aldrich, Germany
Tris Base	Merck, Germany
Tris-HCl	Sigma-Aldrich, Germany
Triton X100	Carl Roth, Germany
Trypan blue	ThermoFisher, USA
Trypsin	Sigma-Aldrich, Germany
Tween 20	Sigma-Aldrich, Germany
Trypsin-EDTA	Sigma-Aldrich, Germany

3.1.2 Enzymes and enzyme buffers

Table 2: Enzymes and enzyme buffers

Name	**Source**
5× Green GoTaq reaction buffer	Promega, Germany
DNAase I	Sigma-Aldrich, Germany
GoTaq G2 DNA polymerase	Promega, Germany
Pronase E	Sigma-Aldrich, Germany
Proteinase K (20 mg/mL)	Sigma-Aldrich, Germany
DAB substrate solution	Dako, USA

3.1.3 Primers

Table 3: Primers

Name	Sequence
Mouse Vimentin-F	CGGCTGCGAGAGAAATTGC
Mouse Vimentin-R	CCACTTTCCGTTCAAGGTCAAG
Mouse TIMP2-F	CTGGACGTTGGAGGAAAGAAG
Mouse TIMP2-R	CTGGGTGATGCTAAGCGTGTC
Mouse CTGF-F	GACCCAACTATGATGCGAGCC
Mouse CTGF-R	CCCATCCCACAGGTCTTAGAAC
Mouse Col1a2-F	GTAACTTCGTGCCTAGCAACA
Mouse Col1a2-R	CCTTTGTCAGAATACTGAGCAGC
Mouse ACTA2-F	GTCCCAGACATCAGGGAGTAA
Mouse ACTA2 R	TCGGATACTTCAGCGTCAGGA
Mouse MMP1-F	CTTCTTCTTGTTGAGCTGGACTC
Mouse MMP1-R	CTGTGGAGGTCACTGTAGACT
Mouse MMP2-F	CAAGTTCCCCGGCGATGTC
Mouse MMP2-R	TTCTGGTCAAGGTCACCTGTC
Mouse MMP9-F	GGACCCGAAGCGGACATTG
Mouse MMP9-R	CGTCGTCGAAATGGGCATCT
Human SMC4-F	TTGTCATGCACTGGACTACATTG
Human SMC4-R	TTTTTCGCCCATACAGCCATC
Human SLC6A1-F	GGGTATGGAAGCTGGCTCCTA
Human SLC6A1-R	AGGGGTTGTCGCACTGTTTC
Human βactin-F	GGGAAATCGTGCGTGACATTAAG
Human βactin-R	TGTGTTGGCGTACAGGTCTTTG

All oligonucleotides were purchased from metabion international AG

3.1.4 gRNA oligonucleotides

Table 4: gRNA oligonucletides

Name	Sequence
HGF-fl Forward	TGACTACGCTGTTCATTCAAGTGC
HGF-fl Reverse	CCATTTCTTCAGAGGCAGATGC
Stab2Cre Forward	AAGCTGAACAACAGGAAATGGTTC
Stab2Cre Reverse	GGAGATGTCCTTCACTCTGATTCT

All oligonucleotides were purchased from metabion international AG

3.1.5 Nucleic acid and protein ladders

Table 5: Nucleic acid and protein ladders

Name	Source
Ribo Ruler high range RNA ladder	ThermoFisher, USA
Page Ruler Pre-stained Protein ladder	ThermoFisher, USA
GeneRuler DNA 10 kb ladder	ThermoFisher, USA
1 kb DNA ladder	New England Biolabs, Germany
100 bp DNA ladder	New England Biolabs, Germany

3.1.6 Antibodies

Table 6: Antibodies

Name	Source
Anti-CD31 (Ms, Sw) from Rat (SZ31)	Dianova, Germany
Donkey Fab anti-Rabbit IgG (H+L)-Alexa Fluor 488	Dianova, Germany
Donkey Fab anti-Rat IgG (H+L)-Alexa Fluor 594	Dianova, Germany
AQP4 (D1F8E) Rabbit mAb	Cell Signaling Technology, USA
Rabbit Anti-Mouse Lyve-1	Dianova, Germany
Mouse Anti-Human CD31	Dako, USA

Rat anti-Mouse Fc gamma RIIB/CD32b	R&D Systems, USA
HGF Antibody (7-2) - BSA Free	Novas Biologicals, USA
anti-CD11b microbeads	Miltenyi Biotec, Germany
anti-stabilin-2 (FITC) antibody	MBL International, USA
anti-cd11b (Pacific blue) antibody	BioLegend, USA
phospho-Smad-3 antibody	Abcam, UK
total-Smad-3 antibody	Abcam, UK
TIMP1 antibody	Cell Signaling Technology, USA
Phospho-PI3 Kinase antibody	Cell Signaling Technology, USA
MMP-2 antibody	Cell Signaling Technology, USA
Phospho-Akt antibody	Cell Signaling Technology, USA
DiI-Ac-LDL	Cell applications, USA
Phospho-PI3 Kinase p85 (Tyr458)/p55 (Tyr199) Antibody	Cell Signaling Technology, USA

3.1.7 Culture media and supplements

Table 7: Culture media and supplements

Name	**Source**
Cell culture water	Sigma-Aldrich, Germany
DMSO	Sigma-Aldrich, Germany
Dulbecco's Modified Eagle's Medium (DMEM)	Sigma-Aldrich, Germany
GlutaMax	Gibco, UK
MEM non-essential amino acids 100×	Sigma-Aldrich, Germany
Opti-MEM	Gibco Life Technologies, USA
Phosphate-buffered saline (PBS)	Sigma-Aldrich, Germany

3.1.8 Laboratory equipment

Table 8: Laboratory equipment

Name	Source
Real-Time PCR System	Applied Biosystems, Germany
Autoclave Systec	Systec, Germany
Automated Microtome	Leica, Germany
Automated Vacuum Tissue Processor	Leica, Germany
Axio Observer Z1 Microscope	Carl Zeiss Jena GmbH, Germany
Axiovert 100	Carl Zeiss Jena GmbH, Germany
Bioruptor Ultrasonic device	Diagenode, Belgium
Cell incubator	Eppendorf, Germany
Corning Stripettor Plus Pipetting Controller for 2-25ml pipettes	Corning Inc., USA
Eppendorf Centrifuge	Eppendorf, Germany
Glass ware (Beaker glass, Erlenmeyer flask, graduated cylinder)	Schott Duran, Germany
Heating Block	Kleinfeld Labortechnik, Germany
Ice Maker	Ziega, Germany
LightCycler 480 II	Roche, Germany
Microplate Reader	Berthold Technologies, Germany
Microplate Washer	Tecan, Switzerland
Microwave Oven	Siemens, Germany
Multifuge 3S-R (for Falcons and Plates)	Heraeus Kendro, Germany
NanoDrop 1000 Spectrophotometer	ThermoFisher, USA
Optimax X-Ray Film Processor (Developing machine for Western Blot films)	Protec, Germany
PH Level I (pH-meter)	WTW inoLab, Germany
Purelab (for ddH_2O)	Elga, UK
Sterilgard Hood	ThermoFisher, USA
Tissue Embedder	Leica, Germany
Trans-Blot SD Semi Dry Transfer Cell	Biorad Laboratories, Germany

Vortex-Genie 2	Scientific Industries, USA

3.1.9 Kits

Table 9: Kits and equipments

Name	Source
20G needle: Neolus	Becton and Dickinson Company, USA
7500 fast real-time PCR cycler	Life Technologies, USA
Accu-jet pro pipetting robot	Brand, Germany
ALT Elisa Kit	Sigma-Aldrich, Germany
Automated Vacuum Tissue Processor	Leica, Germany
Axio Observer Z1 Microscope	Carl Zeiss Jena GmbH, Germany
BCA Protein Assay Kit	ThermoFisher, USA
Blue light table	Serva, Germany
Camera AxioCam MR (Axiovision)	Carl Zeiss Jena GmbH, Germany
Cell counting chamber: Neubauer improved	Brand GmbH, Germany
Centrifuges	Eppendorf, Germany
DNeasy Blood and tissue kit	Qiagen, Germany
Electrophoresis system (buffer, chamber, gel trays, combs)	Biorad Laboratories, Germany
Electroporation generator	Biotechnologie GmbH, Germany
Freezer -20°C	ThermoFisher, USA
Freezer -80°C	ThermoFisher, USA
Gel documentation imaging system Quantum ST5	Vilber Lourmat, Germany
Gel electrophoresis chamber + power adapter	Biorad Laboratories, Germany
Hera Safe clean bench	Heraeus Instruments, Germany
Ice machine	Ziega, Germany
Incubator Steri-cycle CO_2	ThermoFisher, USA
LightCycler 480 Probes Master	Roche, Germany
Microwave oven	Siemens, Germany
Mini centrifuge “perfect spin mini”	Peqlab Biotechnologie, Germany

Mr. Frosty freezing container	ThermoFisher, USA
Orbital shaker	ThermoFisher, USA
PCR cycler "DNA Engine DYAD, PTC0220"	Biorad Laboratories, Germany
PCR cycler "peqStar"	Peqlab Biotechnologie, Germany
Pipettes "Pipetman 10 µL, 200 µL, 1000 µL"	Corning Inc., USA
QuantiTect Reverse Transcription Kit	Qiagen, Germany
RNeasy Mini Kit	Qiagen, Germany
Refrigerator 4℃	Beko, Germany
Rocker shaker	Uniequip, Germany
Syringe filter (0.22 µM)	Berrytec, Germany
Table centrifuge	Sigma-Aldrich,Germany
Vortex mixer	Scientific industries, USA
Water bath	Memmert, Germany

3.1.10 Buffers and solutions

Table 10: Buffers and solutions

Type	Components	Amount
Electrophoresis buffer 10×	Tris $C_2H_5NO_2$ SDS ddH_2O	30 g 144 g 10 g Fill up to 1 L
SDS 10%	SDS ddH_2O	10 g Fill up to 100 mL
TAE 10×	Tris 0.5 M EDTA $C_2H_4O_2$ ddH_2O	242 g 100 mL 57.1 mL Fill up to 5 L
TBE 10×	Tris H_3BO_3 EDTA ddH_2O	545 g 275 g 39.2 g Fill up to 5 L
TE buffer 1×	Tris-HCl EDTA ddH_2O	0.158 g 0.029 g Fill up to 100 mL
Loading Buffer 5×	Trisma base Glycine SDS ddH_2O	150 g 720 g 25 g Fill up to 5 L

Transblot Buffer 10×	Trisma base Glycine ddH2O	58.15 g 29.28 g Fill up to 1 L
SDS lysis Buffer 1×	Glycerol 10% SDS 0.5 M Tris-HCl pH 6.8 0.5% Bromophenol Blue 14.3 M β-ercaptoethanol ddH_2O	7.5 mL 15 mL 6.25 mL 1 mL 2.5 mL Fill up to 50 mL
Tris Buffered Saline (TBS) 10×	Trisma base NaCl ddH_2O Adjust pH to 7.4 with ddH_2O	12.1 g 85 g 800 mL 5M HCl Fill up to 1 L
Citrate Buffer 20×	Citric acid (Monohydrate) Adjust pH to 6.0 with ddH_2O	21 g 5M NaOH Fill up to 500 mL
TBSA 1×	10 × TBS BSA ddH_2O	100 mL 1 g Fill up to 1 L
Phosphate Buffered Saline (PBS) 10×	Phosphate Buffered Saline ddH_2O	95.5 g Fill up to 1 L
Hank's Balanced Salt Solution (HBSS)	NaCl $Na_2HPO_4 \cdot 12H_2O$ $NaH_2PO_4 \cdot 2H_2O$ KCl KH_2PO_4 $MgSO_4$ $CaCl_2$ D-glucose $NaHCO_3$ ddH_2O	8 g 0.126 g 0 g 0.4 g 0.06 g 0.098 g 0.14 g 1 g 0.35 g Fill up to 1 L
Enzyme buffer solution 1×	NaCl KCl $NaH_2PO_4 \cdot H_2O$ Na_2HPO_4 HEPES $NaHCO_3$ $CaCl_2 \cdot 2H_2O$ ddH_2O	8 g 0.4 g 0.08817 g 0.12045 g 2.38 g 0.35 g 0.56 g Fill up to 1 L
Gey´s Balanced Salt Solution B (GBSS/B)	NaCl KCl $MgCl_2 \cdot 6H_2O$ $MgSO_4 \cdot 7H_2O$ Na_2HPO_4 KH_2PO_4 Glucose $CaHCO_3$ $NaHCO_3$ ddH_2O	8 g 0.37 g 0.21 g 0.07 g 0.0596 g 0.03 g 0.991 g 0.227 g 0.225 g Fill up to 1 L

Washing buffer (TBST)	10 × TBS Tween 20 ddH_2O	100 mL 0.5 mL Fill up to 1 L
Gey´s Balanced Salt Solution A (GBSS/A)	KCl $MgCl_2 \cdot 6H_2O$ $MgSO_4 \cdot 7H_2O$ Na_2HPO_4 KH_2PO_4 Glucose $CaHCO_3$ $NaHCO_3$ ddH_2O	0.37 g 0.21 g 0.07 g 0.0596 g 0.03 g 0.991 g 0.227 g 0.225 g Fill up to 1 L

3.1.11 Consumables

Table 11: Consumables

Name	Source
Carbon dioxide gas cylinders, 200 bar (CO_2)	Westfalen AG, Germany
Cell culture plates	Corning Inc., USA
CellStar tubes (15 mL and 50 mL)	Greiner Bio-One, Germany
Cloning rings	Brand, Germany
Cover slips	Menzel, Germany
Cryo-vials	Corning Inc., USA
Filter pipette tips “Fisher brand Sure One”	Fisher Scientific, USA
Glass Pasteur pipettes	Brand, Germany
Micro loader Tip	Eppendorf, Germany
Nitrogen gas cylinders, 200 bar (N_2)	Westfalen AG, Germany
Oxygen gas cylinders, 200 bar (O_2)	Westfalen AG, Germany
PCR tubes 0.2 ml 8-strip PCR tubes	Starlab, Germany
Petri dishes	Greiner Bio-One,Germany
Pipette tips	Brand, Germany
Plastic pipettes “Costar Stripette” (1- 50 ml)	Corning Inc., USA
Reaction tubes (1.5 mL and 2 mL)	Starlab, Germany
Sterile filter 0.22 µM	Berrytec, Germany
Syringes	BD Bioscience, France

Tissue culture plates (10 cM, and 6-, 12-, 24-well)	Corning Inc., USA
Tubes (15 mL, 50 mL)	Corning Inc., USA

3.1.12 Software and online tools

Table 12: Software and online tools

Name	Source
R (programming language)	https://www.r-project.org/
Genome database “Ensembl”	https://www.ensembl.org/index.html
Microscope software “Axio Vision”	Carl Zeiss Jena GmbH, Germany
GraphPad Prism Version 8.4.3	https://www.graphpad.com/scientific-software/prism/
ImageJ	https://imagej.nih.gov/ij/download.html
Primer bank	https://pga.mgh.harvard.edu/primerbank/
Primer blast	https://www.ncbi.nlm.nih.gov/tools/primer blast/

3.1.13 Veterinarian medicinal products and equipment

Table 13: Veterianarian medicinal products and equipement

Name	Sequence
Disposable scalpels	B. Braun AG, Germany
Needle holder, Matthieu, 20 cM	Omega Medical, Germany
Surgical drape	B. Braun AG, Germany
Surgical gloves, Peha-taft latex	Omega Medical, Germany
Surgical instruments	HBH Medizintechnik, Germany
Cellulose swabs	B. Braun AG, Germany
Carbon tetrachloride (CCl_4), 100 mL	Sigma-Aldrich, Germany
Syringes (1 mL, 5 mL, 10 mL, 20 mL)	B. Braun AG, Germany
Olive Oil	Sigma-Aldrich, Germany
Collagenase D	Sigma-Aldrich, Germany

3.2 Methods

3.2.1 $HGF^{LSEC-KO}$ mouse model

HGF knockout in LSECs ($HGF^{LSEC-KO}$: $HGF^{fl/fl}$ and Stab2-$iCre^{tg/wt}$ or $HGF^{fl/fl}$ and Stab2-$iCre^{tg/tg}$) was achieved by crossing Stab2-$iCre^{tg/tg}$ with $HGF^{fl/fl}$ mice (Phaneuf, Moscioni et al. 2004). The animal experiments were approved by the animal ethics committee (Regierungspraesidium Karlsruhe) and institutionally by the District Government of Upper Bavaria and performed under institutional guidelines (ROB-55.2-2532. Vet_02-18-64). All animals were housed and bred under specific pathogen free (SPF) conditions in the animal facility (Zentrum für Präklinische Forschung, ZPF – TranslaTUM). The mouse experiments performed abide by federal animal regulations. For this study, we were allowed to breed $HGF^{LSEC-KO}$ mice for all the mentioned experiments.

3.2.2 Mouse liver fibrosis model

Carbon tetrachloride (CCl_4) (Tetrachlorkohlenstoff, 289116, Sigma-Aldrich, Inc, SAFC, diluted in olive oil, 1:7) was used in this part. Male mice aged at 10 weeks, weighing from 20 to 26 g, were given 0.5 mg/kg CCl_4 or control phosphate buffered saline (PBS) solution by intraperitoneal injection (i.p.). Mice were injected twice a week for 4, 6, and 8 weeks, respectively. Mice were sacrificed 24 hours after the last CCl_4 administration.

3.2.3 Sample harvest and processing

Mice were euthanised by isoflurane and cervical dislocation. Cardiac puncture was used to obtain blood. Liver samples were collected in liquid nitrogen and kept at -80°C for

subsequent protein and RNA extraction, and another portion of liver tissue was collected in fixed in 4% paraformaldehyde for 24 hours at room temperature. For paraffin blocks, samples were transferred into PBS, dehydrated in a series of graded alcohol solutions, embedded in paraffin, and then sectioned into 3 μM slices.

3.2.4 Genotyping

- The primer was diluted to 20 μM. Buffer A and buffer B were prepared for following experiments.

Type	Components	Amount
Buffer A	NaOH EDTA ddH_2O	0.05 g 0.0038 g Fill up to 50 mL
Buffer B	Tris 5N HCl ddH_2O	0.24228 g Adjusted to 5.5 Fill up to 50 mL

- Mouse biopsy and 150 μL Buffer A were put into an EP tube, which was then placed in a metal bath at 100°C for 60 minutes with a constant flick (350 rpm). After the tissue dissolved completely and the solution cooled down to room temperature, 150 μL Buffer B was added and mixed gently, then centrifuged at 4,000 rpm for 3 minutes, where supernatant was collected and stored at 4°C. Next steps are per the following protocols.

PCR amplification mix system (10 μL):

Taq mix	5 μL
Upstream primer	0.5 μL
Downstream primer	0.5 μL
DNA template	2 μL
ddH_2O	2 μL

PCR amplification program:

95℃	5 minutes	
95℃	30 seconds	40 cycles
58℃	30 seconds	
72℃	45 seconds	
72℃	10 minutes	
4℃	Forever	

3.2.5 Agarose gel electrophoresis

1.5 ± 0.5% agarose supplemented with 4 μL ethidium bromide (EB, Gel staining, 5 μL per 100 mL, ThermoFisher) was prepared. It was then diluted with 100 mL 1× TAE and heated in the microwave oven for 5 minutes at high heat. After the gel cooled down to room temperature, DNA fragments were loaded and run by agarose gel electrophoresis (10 μL/well, 200 V constant voltage for 25 minutes). Subsequent imaging of DNA fragments was illumination under UV light (254–366 nm) with the referred documentation system. The positions of the imaging bands in HGF mice are as follows:

HGF-fl	target mutant: 500 bp
	target wild type: 430 bp
Stab2-iCre	target: 400 bp

3.2.6 Western blot

- Extraction of cell and tissue proteins.

For cells, before digesting the cells, the supernatant was discarded, and washed three times with 1× PBS. Next, corresponding RIPA lysis solution was added (add 1:100 protease inhibitor) according to the size of the culture dish and placed on ice for 1–2 minutes. The cell scraper was performed to hang the cells in the culture dish. The final solution was transferred to a 1.5 mL EP tube, placed in ice for 30 minutes of lysis, and centrifuged at 12,000 rpm for 10 minutes at 4°C. Then the supernatant was aspirated to a fresh 1.5 mL EP tube.

For tissue, it was cut into pieces the size of soybeans. An appropriate amount of RIPA lysis buffer was added and ground completely with the shaking apparatus. Then it was placed in ice for lysis for 30 minutes and centrifuged at 12,000 rpm at 4°C for 10 minutes. Finally, the precipitation was discarded, and the supernatant was aspirated to a fresh 1.5 mL EP tube.

- The BCA Protein Assay Kit was employed to detect the above protein concentration. The BCA reaction reagent was diluted into a working solution according to the instructions (solution A: solution B, 50:1), mixed thoroughly and placed in ice, protected from light. Then, 5 μL of protein solution was diluted with 100 μL RIPA lysis buffer, where the diluted protein and BCA standard samples were added to the 96-well plate, mixing with 200 μL of BCA working solution in each well. The 96-well plate was

incubated and protected from light at 37°C for 30 minutes. The OD value of each well was detected in the microplate reader instrument (the wavelength of absorbed light set to 562 nm). Based on absorption values, the standard curve was drawn, and the protein concentration in each well was calculated according to the formula.

- Separation of protein electrophoresis steps.

1. Protein denaturation

The final calculated protein solution was balanced with RIPA lysis buffer and the equal volume of protein SDS-loading buffer (2×). It was next denatured in a metal bath at 100°C for 5–10 minutes, and quickly cooled down in ice. After centrifugation, the samples were either stored in a -80°C freezer or proceeded to the following steps.

2. Polyacrylamide gel preparation

The glass plate was fixed on the gel rack according to the required concentration of separating gel (10 mL). It was then added to the two-layer glass plate after mixing evenly (10 mL of ddH_2O was used for leak detection). An appropriate amount of isopropanol is used to flatten the separating gel (6 mL). The glass plate was kept at room temperature for about 15 minutes until the separation gel was completely solidified and the upper layer of isopropanol was discarded (filter paper was used to absorb residual isopropanol). After preparing the stacking gel, it was transferred to the top layer of the solidified separation gel. The protein loading comb was next inserted into the gel, leaving it at room temperature for about 10 minutes to solidify completely.

Separating gel (10 mL)	8%	10%	12%
Acrylamide 30%	2.7 mL	3.3 mL	4 mL
Tris-HCL 1.5M pH8.8	3.8 mL	3.8 mL	2 mL
10% APS	100 μL	100 μL	3.8 μL
10% SDS	100 μL	100 μL	100 μL
TEMED	6 μL	6 μL	100 μL
ddH_2O	3.3 mL	2.7 mL	2 mL

Stacking gel (6 mL)	5%
Acrylamide 30%	1.0 mL
Tris-HCL 1.5M pH6.8	0.75 mL
10% APS	60 μL
10% SDS	60 μL
TEMED	6 μL
ddH_2O	4.1 mL

3. Protein electrophoresis

The above gel glass plate was put into the electrophoresis tank, filled with the 1× protein electrophoresis solution prepared in advance. After the sample loading comb was removed, 40 μg of protein was added to the protein lane by using a pipette. Next, electrophoresis adapters were assembled, where electrophoresis was started at 80 V for around 20 minutes. When the protein markers were separated, the voltage was adjusted to 120 V. When the protein markers were close to the bottom of the glass plate, the electrophoresis was stopped.

- Western blotting

1. After carefully removing the glass plate from the electrophoresis tank, the black end

were put in an order in the transfer plate according to the “sandwich” principle—filter paper, gel, NC membrane (or PVDF membrane—requires methanol activation), filter paper—white end and air bubbles must be removed carefully between the layers.

2. The transfer rack, the film, and transfer tank were assembled correctly and filled with the blotting buffer. Then the entire transfer tank was kept in a blotting of 300 mA constant current and placed in an ice environment, while the immunoblotting and blotting times were adjusted according to the molecular weight.

- Antigen blocking, antibody incubation and chemiluminescent detection

After the NC membranes obtained above were trimmed, they were washed three times with 1× TBST and placed in the prepared protein blocking solution (5% non-fat milk) for 1 hour at room temperature on a shaker for blocking. Next, they were immersed in the antibody diluent (according to the antibody instructions) and shaken at 4°C overnight. The second day, the NC membranes were washed three times with 1× TBST on a shaker at room temperature (10 minutes for each), then incubated with the secondary antibody (dissolved in 5% non-fat milk) at room temperature for 1 hour. After that, they were washed with 1× TBST three times (10 minutes for each) on a shaker. The NC membranes were covered with the working solution directly, which is provided by the chemiluminescence kit (A solution: B solution, 1:1 volume preparation), and an imaging instrument (Analytik Jena) was applied to capture the target protein. Finally, Image J software was used for grey value quantification and the following statistical analysis.

3.2.7 RNA extraction, reverse transcription, and quantitative real-time PCR (qRT-PCR)

- For cells, the medium in the culture dish was completely discarded, an appropriate amount of Trizol (for example, add 200 μL Trizol to 6 cm diameter culture dish) was added. Then the cell lysate was transferred into a 1.5 mL EP tube.
- For tissue, the frozen tissue was removed from the -80°C freezer, cut into soybean-size and placed in a 1.5 mL EP tube. Together with corresponding Trizol (100 mg of tissue is dissolved in 1 mL of Trizol) and steel balls, the EP tube was placed in a tissue grinding apparatus for 90 seconds. After a complete lysis, the supernatant was aspirated and transferred to a new 1.5 mL EP tube.
- Around 1/5 Trizol volume of chloroform (about 100 μL) was added to the tubes and kept for another 3 minutes. After centrifuging at 12,000 rpm at 4°C for 10 minutes, the upper colourless aqueous phase (the RNA components were located) was pipetted into a new 1.5 mL EP tube. An equal volume of isopropanol was mixed in this tube completely and kept at room temperature for 3–5 minutes. After centrifuging at 12,000 rpm at 4°C for 10 minutes, the supernatant was discarded, and a small amount of white insoluble precipitates were retrieved from the bottom of the tube. 1 mL of pre-cooled 75% ethanol was used to wash the white precipitate and shake it gently three times. Next, it was centrifuged at 8,000 rpm at 4°C for 5 minutes. After discarding supernatant, the EP tube was inverted on absorbent filter paper for 3–5 minutes. Pre-cooled DNase/RNase-Free water (range from 60–80 μL) was used to completely dissolve the insoluble precipitates at the bottom of the tube. Nano Drop 2000 was applied to detect the concentration of purified RNA, and then reverse transcription reaction was performed.

Finally, RNA was frozen at -80℃.

- The RNA reverse transcription reaction was next. For the removal of the genome DNA contamination, 1 μg template total RNA was mixed with DNase solution (2 μL 7× gDNA wiper Mix, adjusted with RNase free ddH_2O to 14 μL) and placed in a constant temperature metal bath at 42°C for 2 minutes. Next, for preparation of cDNA reverse reaction mix, 14 μL of the above-obtained mixed solution was added with 1 μL RT primer mix, 4 μL 5× Quantiscript RT buffer, and 1 μL Quantiscript Reverse Transcriptase. This reaction mix was then put through 50℃ for 15 minutes, 85℃ for 2 minutes, and 4℃ forever.

Note: For templates with high GC regions, the reaction temperature in step 1 can be set to 55°C, which can improve the yield of cDNA. The final cDNA product should avoid repeated freezing and thawing. If it is not used temporarily, it can be stored in a freezer at -80°C.

- After that, the following reaction mix system was made for real-time fluorescent quantitative PCR detection of target genes.

qPCR reaction system mix

ChamQ SYBR qPCR Master Mix (2×)	5 μL
ddH_2O	3.5 μL
Primer Forward (10 μM)	0.25 μL
Primer Reverse (10 μM)	0.25 μL
cDNA product template	1 μL
Total reaction volume	10 μL

Next, the reaction system mix was processed in a real-time PCR reaction program as follows:

Step 1	Denaturation	Repeat: 1	95℃	30 seconds	
Step 2	Cycle reaction	Repeat: 40	95℃	10 seconds	
			60℃	30 seconds	Reading
Step 3	Melting curve	Repeat: 1	95℃	15 seconds	
			60℃	60 seconds	
			95℃	15 seconds	

Note: If the structure of the cDNA template is complex, the time of Step 1 can be extended to 3 minutes, which can improve the denaturation effect. If the amplicon exceeds 300 bp, the extended time in Step 2 can be increased to 60 seconds, which can improve the yield of DNA. Quantitative real-time PCR (qRT-PCR) was finally implemented under the LightCyclerTM480 system with the SYBR Green 1 Master Kit (Roche Diagnostics, Germany). The calculation of amplification results is based on the final Ct value obtained, which is calculated by using the relative internal parameter quantification method ($2^{-\Delta\Delta Ct}$).

3.2.8 Immunohistochemical staining (IHC)

- Tissue was immersed with PBS and fixed in 4% paraformaldehyde for at least 24 hours before the dehydration procedure. Then it proceeded to paraffin-embedded sectioning.
- After obtaining the paraffin tissue sections, they were placed on a 70°C baking

oven for 30 minutes and quickly moved to roticlear for complete dewaxing.

- For dewaxing and hydration steps, sections were immersed in roticlear I for 20 minutes, roticlear II for 20 minutes, absolute ethanol for 5 minutes, 96% ethanol for 5 minutes, 70% ethanol for 5 minutes, 50% ethanol for 5 minutes, and tap water for 10 minutes.

- Antigen retrieval solution was obtained by diluting 20× sodium citrate retrieval solution with 1× PBS in advance (0.01 M, pH 6.0). The sections were immersed in 1× antigen retrieval solution and placed in a microwave oven on high for 2 minutes until fully boiled and at medium-low level for 15 minutes. After cooled to room temperature, the sections were washed three times with 1× PBS (5 minutes each time).

- Next, deactivation of endogenous peroxidase blocking agent, containing 3% hydrogen peroxide, was used to immerse the sections for 15 minutes. Then it was washed three times with 1× PBS (5 minutes each time).

- The tissue sections were incubated with blocking buffer (10% BSA solution or 10% goat serum) at room temperature for 1 hour, then the blocking solution was thrown off without washing. Primary antibody was diluted with 1% BSA solution (dilution ratio according to the antibody instructions) and used to incubate the sections in a dark box at 4°C overnight.

- The next day, the tissue sections were washed three times with 1× PBS (5 minutes each time secondary antibody diluted with 1% BSA added dropwise. Together with the sections, they were incubated for 1 hour at room temperature, and washed three times with 1× PBS (5 minutes each time).

- Next, the sections proceeded with DAB chemiluminescent detection. DAB

working liquid was prepared according to the instructions, it was dripped on the sliced tissue, which was observed under an optical microscope to control the colour development time. It was rinsed with tap water for 10 minutes.

- The sections were stained with hematoxylin for 30–60 seconds and rinsed with tap water for 10 minutes. Next, they sere dehydrated with 50% ethanol for 1 minute, 70% ethanol for 1 minute, 96% ethanol for 1 minute, absolute ethanol for 1 minute, roticlear I for 3 minutes, and roticlear II for 3 minutes, respectively.
- Sections were finally mounted with permanent mounting medium.

3.2.9 Cell culture, passage, and cryopreservation

- For resuscitation of frozen cells, the cryopreserved cells in liquid nitrogen were quickly placed in a 37°C constant temperature water bath. Then 5 mL of cell culture medium was added and transferred to 15 mL tube. After centrifuging at 1,000 rpm for 5 minutes, the supernatant was discarded and an appropriate medium was added to resuspend and seed in the dish.
- The cells used in this experiment were cultured in DMEM medium (10% FBS, 1:100 streptomycin/penicillin double antibody) and placed in a 5% CO_2, 37°C incubator. The medium in the culture dish was discarded and washed three times with 1× PBS before digested with trypsin for around 3 minutes. Then cells were transferred to a 15 mL tube and centrifuged at 1,000 rpm for 5 minutes. The supernatant was discarded, the cells were resuspended in complete medium, and a cell counter was used to calculate the cell number before seeding.
- For cell cryopreservation, after digesting with trypsin, cells were centrifuged at 1,000 rpm for 5 minutes. The supernatant was discarded, and cells were resuspended

with cell freezing medium (10% DMSO, 90% serum), transferred to cryopreservation tubes, sealed with parafilm, and placed in a cell cryopreservation box (4℃ for 30 minutes, -20 ℃ for 1 hour, -80 ℃ overnight, and then transferred to a liquid nitrogen tank for long-term storage after 48 hours).

3.2.10 Protein co-immunoprecipitation (CO-IP)

- Firstly, an appropriate IP Lysis Buffer was added to the tissue protein. After the tissue was completely lysed, the protein was placed in a 1.5 mL EP tube, kept on ice for 30 minutes, and centrifuged at 12,000 rpm for 10 minutes at 4℃. A BCA kit was used to balance the protein concentrate and volume to the same level.
- Then a certain amount of antibody (according to the antibody instructions) was added to the sample tubes. For the positive input control tube, a part of the protein was mixed with the equal volume of 2× protein loading buffer and kept in a metal bath at 100℃ for 5 minutes. For the negative control tube, an appropriate anti-IgG antibody (according to the antibody instructions) was added to a part of the protein. All samples and negative tubes were then sealed with parafilm and placed on a rotating windmill at 4℃ overnight.
- For protein A/G conjugated antibody step, 50 μL Protein A/G (ThermoFisher) was added to each tube (shake well before adding) and sealed with parafilm. Then it was put back into the rotating windmill at 4℃ for 3 hours.
- All the EP tubes were centrifuged at 5,000 rpm for 5 minutes at 4℃, the supernatant was discarded, 300 μL IP Lysis buffer was added, then centrifuged at 5,000 rpm for 5 minutes at 4 ℃. This step was repeated two more times.
- Next was protein denaturation. An equal volume of 2× protein loading buffer

was added to the precipitation, put in a metal bath at 100°C for 5 minutes, and placed on ice immediately. Then either protein electrophoresis was performed or stored in a -80°C freezer.

3.2.11 Hematoxylin eosin staining (H&E)

- The tissue was fixed in 4% paraformaldehyde for 24 hours, followed by dehydration, paraffin embedding, and paraffin-embedded sectioning.
- The paraffin tissue sections obtained were placed in a baking oven at 70°C for 30 minutes. After the paraffin completely melted, they were quickly immersed in roticlear for dewaxing.
- Slices were next immersed in roticlear for 20 minutes (×3), absolute ethanol for 5 minutes, 95% ethanol for 5 minutes, 85% ethanol for 5 minutes, 75% ethanol for 5 minutes, and tap water for 10 minutes, respectively.
- Cell nuclei were stained with hematoxylin for 30–60 seconds.
- The sections were rinsed with tap water for 5 minutes to remove residual hematoxylin.
- The tissue sections were stained with alcoholic eosin staining for 60 seconds.
- The sections were proceeded with 96% ethanol I for 30 seconds, 96% ethanol II for 30 seconds, 100% ethanol I for 30 seconds, 100% ethanol II for 30 seconds, roticlear I for 30 seconds, and roticlear II for 30 seconds.
- The sections were finally mounted with mounting medium.

3.2.12 Sirius red and Masson blue

1. Sirius red staining

- The paraffin sections were deparaffinised in the heating oven at 75°C for at least

30 minutes.

- The sections were immersed with roticlear for 10 minutes (three times), ethanol series (100%, 100%, 100%, 96%, 70%, and 50%, at 3 minutes each), tap water for 3 minutes, hematoxylin for 1 minute, and tap water for 2 minutes. Next, they were stained with Sirius red solution for 60 minutes.
- The tissue sections were immersed with 30% acetic acid for 1 minute (two times), 96% ethanol for 1.5 minutes (two times), isopropanol for 1.5 minutes (two times), and roticlear for 3 minutes (two times).
- Finally, the slides were mounted with mounting medium.

2. Masson blue staining

- The sections were rinsed with distilled water for 30–60 seconds before staining.
- The sections were stained in hematoxylin for 30–60 seconds and rinsed with washing solution for around 30 seconds.
- An appropriate amount of acid fuchsin slurry was added to the slides for 30–60 seconds of dying and rinsed with cleaning solution for around 30 seconds.
- The sections were immersed with phosphomolybdic acid colour separation solution for colour separation for 6–8 minutes.
- The sections were stained with aniline blue counterstain solution for 5 minutes and rinsed with absolute ethanol.
- The sections were finally mounted for following microscopy.

3.2.13 Hepatic stellate cell (HSC) isolation

- Mice should be at least 6 months old. The following solutions were prepared freshly, including (A) EGTA solution (10 mL per mouse), (B) enzyme solution added

with 0.5 mg/mL pronase E (10 mL per mouse, Merck), (C) enzyme solution added with 0.5 mg/mL collagenase D (20 mL/mouse, Roche), (D) enzyme solution added with 0.3 mg/mL pronase E and 0.3 mg/mL collagenase D and 0.01 mg/mL DNase I (40 mL per mouse, Roche). All the solutions were incubated in a water bath (40°C).

	EGTA-solution pH 7.38	Enzyme-solution pH 7.38
10× HSC-stock solution	1:10	1:10
EGTA	190 mg/L	/
Glucose	900 mg/L	/
$CaCl_2 \cdot 2H_2O$	/	560 mg/L

- Mice were anesthetised with isoflurane and the abdomen was opened. The indwelling baby catheter (purple) was inserted into the inferior vena cava and the portal vein was cut.
- It was perfused (5 mL/min) with enzyme solution (A) for 2 minutes, enzyme solution (B) for 2 minutes, and enzyme solution (C) for 3–4 minutes.
- The liver was taken out and stored on ice in HBSS with foetal bovine serum (FBS) and penicillin/streptomycin. Then the liver was transferred to a petri dish and minced.
- The primary liver cells were transferred into a 200 mL flask and the rest of solution D was added. It was incubated at room temperature with stirring (400 rpm) for 3–5 minutes.
- The digested liver was filtered through sterile nylon mesh sheet (100 µm) and transferred to Falcon tubes (50 mL), centrifuged at 500 g for 7 minutes at 4°C, and the supernatant discarded.
- Each pellet was resuspended in 10 mL of HBSS with 10% FBS and

penicillin/streptomycin containing 30 µl DNase I. Cell suspensions were collected into two Falcon tubes (50 mL).

- HBSS with 10% FBS and penicillin/streptomycin was added up to 50 mL and centrifuged at 500 g for 7 minutes at 4°C.
- Supernatant was discarded and 10 mL HBSS with 10% FBS and penicillin/streptomycin containing 30 µl DNase I was added into the Falcon tube.
- The pellet was resuspended, then HBSS with 10% FBS was added up to 34 mL.
- 13.5 mL Nycodenz solution (8 g/27.5 mL of GBSS/A) was added and mixed well (for 5–6 minutes). Then 11.5–12 mL of the above solution was transferred into four tubes (15 mL).
- 1 mL of HBSS with 10% FBS was laid onto the solution and centrifuged at 1,400 g for 24 minutes at 4°C with no break. Under the layer of clear HBSS is the white layer (stellate cells).
- Stellate cells were transferred to 50 mL tubes and HBSS with 10% FBS was added. The tubes were centrifuged at 500 g for 7 minutes at 4°C.
- The pellet was then resuspended in DMEM, containing 10% FBS, penicillin/streptomycin, and glutamine.
- Cells were counted and seeded in 6-well-plate.

Stock solutions contained 50 mg/mL pronase E, 50 mg/mL collagenase D, 10 mg/mL DNase I, and the 10× HSC stock solution, prepared as follows.

	10× HSC stock solution pH 7.38 (stable at 4°C)
NaCl	80 g/L
KCl	4 g/L
$NaH_2PO_4 \cdot H_2O$	0.882 g/L
Na_2HPO_4	1.2 g/L (1.5 g/L Dihydrate)
HEPES	2.4 g/L
$NaHCO_3$	3.5 g/L

3.2.14 LSEC isolation

LSECs were first magnetically labelled with CD146 MicroBeads (Miltenyi Biotec) and the cell suspension was loaded onto a MACS® Column, which was placed in the magnetic field of a MACS Separator. The magnetically labelled LSECs were retained within the column. The unlabelled cells were run through the separator, which was thus depleted of LSECs. After removing the column from the magnetic field, the magnetically retained LSECs can be eluted as the positively selected cell fraction.

3.2.15 RNA sequencing (RNA-seq) and analysis

The RNA-seq was supported by Thomas Engleitner, Rupert Öllinger, and Roland R. Rad (Institute of Molecular Oncology and Functional Genomics, Department of Medicine II and TranslaTUM Cancer Center, Klinikum rechts der Isar, Technical University of Munich, Germany). Raw count matrices were imported into R and a differential gene expression analysis was conducted using limma. Dispersion estimates were calculated setting the option fitType to parametric using all samples available. A Wald test was conducted to detect differences between genotypes for all available time points. A gene was called significantly regulated if the p-value was below 0.05. Genes regulated in $HGF^{fl/fl}$ mice are shown as a heatmap together with the $HGF^{LSEC\text{-}KO}$

samples.

3.2.16 Statistical methods

This study mainly used statistical software such as GraphPad Prism 8.4 (San Diego, CA) for analysis. Image pro plus V6.0 (Media Cybernetics, Inc. MD) was applied to make quantification of the positive area of staining images. Unless otherwise stated, there were at least three biological replicates for each experiment in this experiment and were expressed as mean ± standard deviation (SD). Unpaired t-tests were used to assess the statistical significance of differences between groups. Pearson's correlation coefficient (r) was calculated to assess correlation.

4 RESULTS

4.1 Establishment of murine liver fibrosis model

A genetically modified HGF ablation in mouse LSECs was achieved by crossing LSEC-specific Stab2 promoter-driven Cre mice (Stab2-iCre) (Koch, Olsavszky et al. 2017) and homozygous $HGF^{ex.5\ flox}$ ($HGF^{fl/fl}$) (Phaneuf, Moscioni et al. 2004). $HGF^{LSEC\text{-}KO}$ embryos did not exhibit any developmental defects and survived healthily to late adulthood (Geraud, Koch et al. 2017). Besides, our former study demonstrated that, in the mice of HGF ablation in LSECs, there is no influence on the liver damage or fibrosis by routine histology staining (H&E, Periodic acid Schiff, and Sirius red) (Zhang, Olsavszky et al. 2020). Thus, it's convincing to perform the subsequent experiment on these mice for liver fibrosis investigation. Carbon tetrachloride (CCl_4) was administrated in male mice aged 10 weeks, weighing from 20 to 26 g, given 0.5 mg/kg CCl_4 by i.p. injection (Figure 2). Mice were injected twice a week for 4, 6, and 8 weeks, respectively, and sacrificed 24 hours after the last CCl_4 administration. After the CCl_4 injection at dynamic time periods, we got a series of multiple degrees of liver fibrosis.

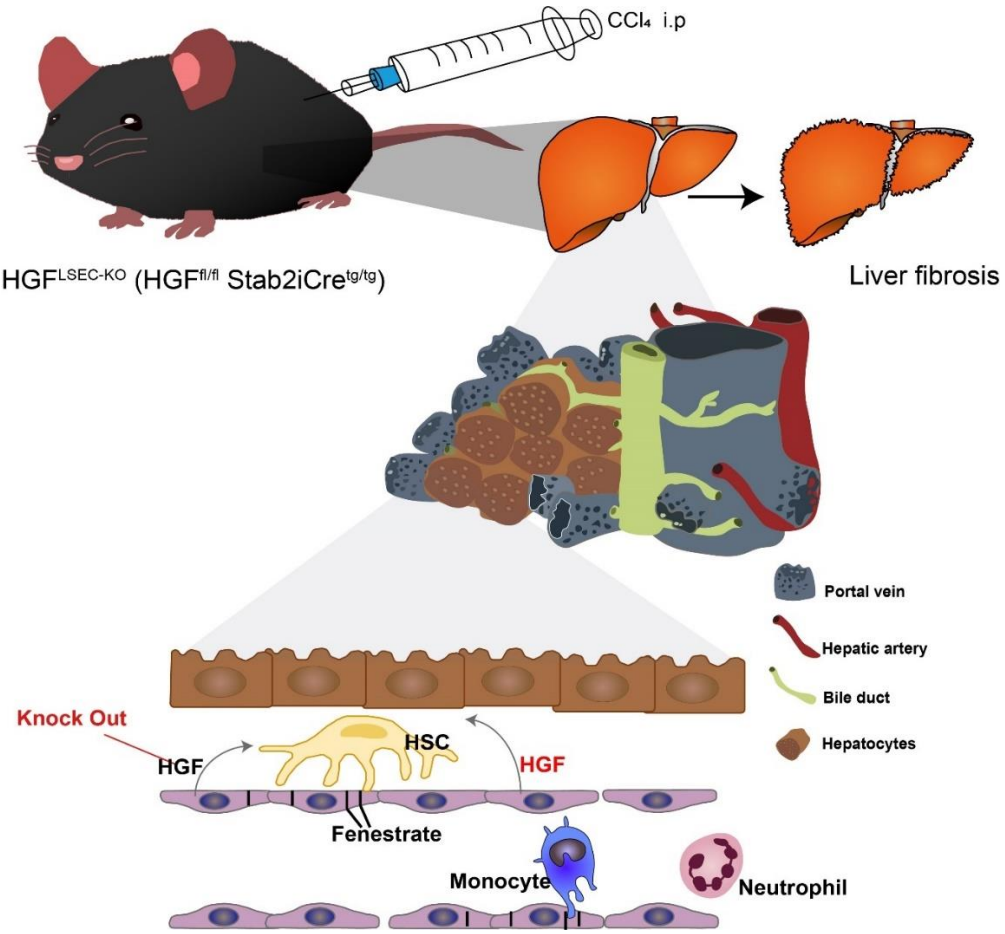

Figure 2. Graphical illustration of genetic modified mouse for this study

$HGF^{fl/fl}Stab2iCre^{tg}$ mice, whose HGF is specifically knockout in LSECs, were achieved and injected with CCl_4 to establish the liver fibrosis model. Compared with the normal mice whose LSEC can express the HGF, $HGF^{LSEC\text{-}KO}$ mice were investigated whether there is a difference in fibrotic severity, fenestration of LSEC and immune cell infiltration.

4.2 HGF ablation in LSECs does not impact severity of liver fibrosis in the late stage, but in the early stage

Based on the frequently used mature establishment of mouse fibrosis model, $HGF^{fl/fl}$ and $HGF^{LSEC\text{-}KO}$ mice were i.p. injected with CCl_4 for the above-mentioned time points. At the 6-week time point, it was found that no impact of HGF deficiency in LSECs on liver fibrosis both in liver tissue morphology and protein level, by fibrosis score of the combination of these two collagen markers. As to the severity of liver fibrosis, it's expectedly found that there is no alteration in liver fibrosis after the deletion of HGF in LSECs (Figure 3A). Similarly, as it comes to the 8-week time point, it was found that

there is still no statistically significant difference between the WT and $HGF^{LSEC-KO}$ mice (Figure 3B).

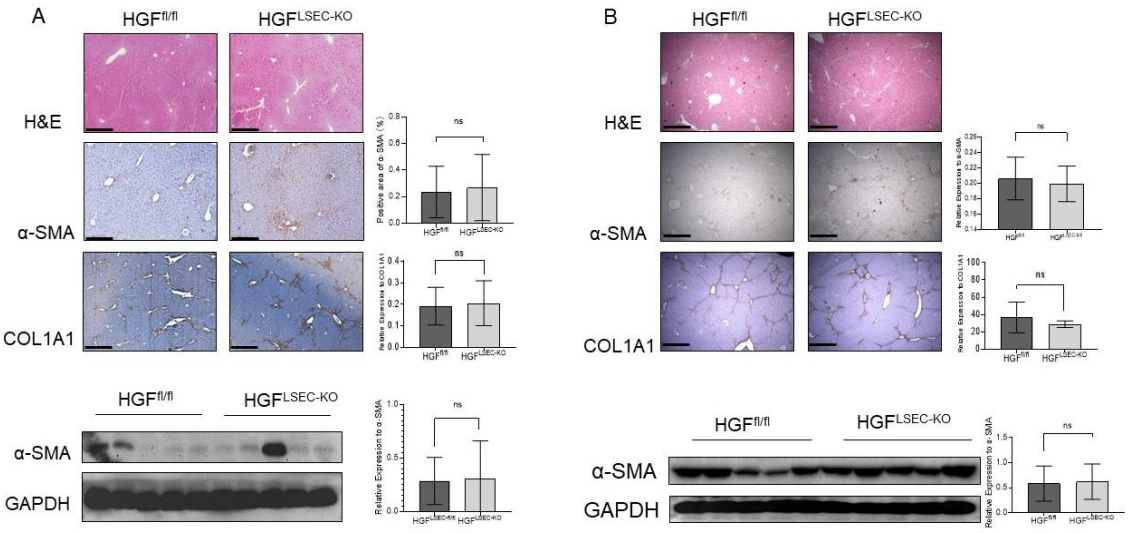

Figure 3. Hepatic angiocrine HGF does not alter severity of liver fibrogenesis in the late stage
(A) All mice were intraperitoneal injected with CCl_4 for 6 weeks (n = 5). H&E staining, IHC staining for αSMA, COL1A1, and western blotting for αSMA. (B) All mice were intraperitoneal injected with CCl_4 for 8 weeks (n = 8). H&E staining, IHC staining for αSMA, COL1A1, and western blotting for αSMA. (scale bar = 500 μM. ns. means no significant)

Next, we shorten the CCl_4-stimulated period to 4 weeks. Interestingly, it was found that the phenotype was significantly located in the liver to body weight ratio (Figure 4A) and liver damage (Figure 4B) after liver fibrosis. In the untreated control groups, there is no difference between $HGF^{fl/fl}$ and $HGF^{LSEC-KO}$ mice.

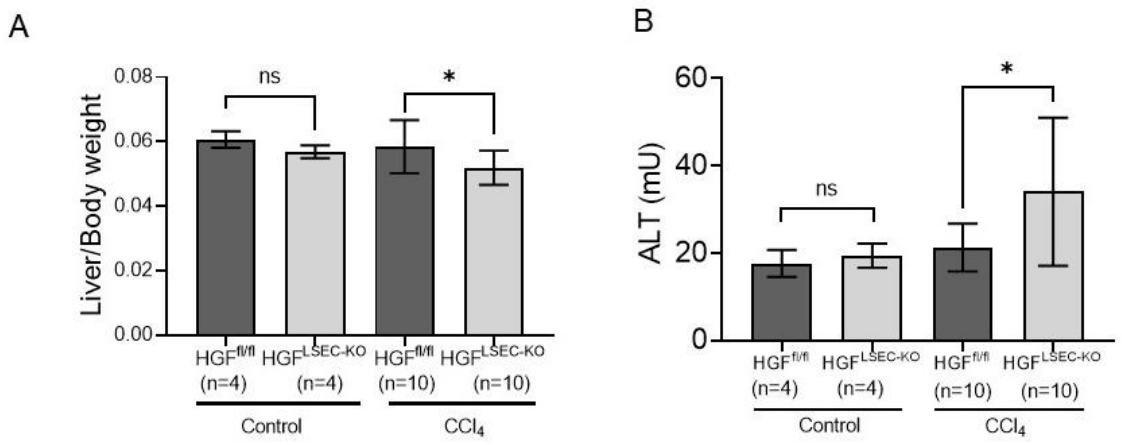

Figure 4. Liver-to-body weight ratio and liver damage among control and liver fibrosis
(A) liver to body weight ratio and (B) serum aminotransferase (ALT) level in $HGF^{fl/fl}$ and $HGF^{LSEC\text{-}KO}$ with untreated control and CCl_4-stimulated liver fibrosis. (ns = no significance, * $p < 0.05$)

As it comes to the liver fibrosis level, one hallmark of this pathology is the deposition of collagen in liver parenchyma. We applied the routine staining method for these experimental mice. By the routine fibrotic staining, intriguingly, for the murine liver fibrosis model, it presented a more severe fibrotic level in the setting of LSEC-specific HGF deficiency (Figures 5A and B). It reveals there is significant morphological changes in inflammation, or depositions of collagens after deletion of HGF in LSECs.

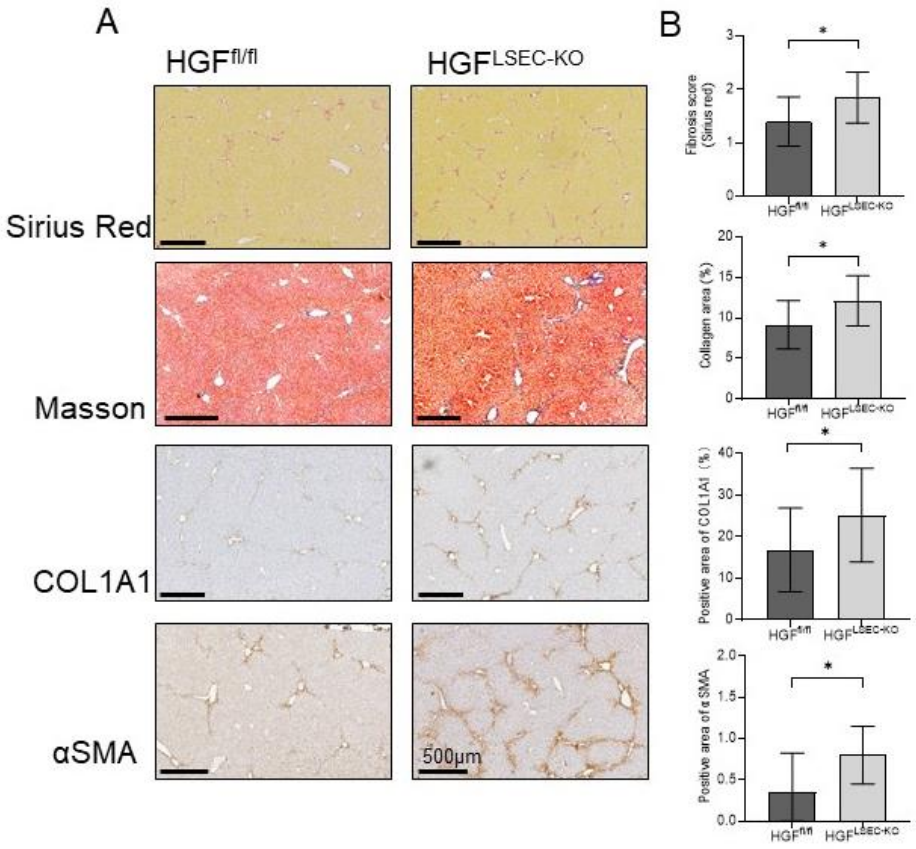

Figure 5. Histological analysis between HGF$^{fl/fl}$ and HGF$^{LSEC\text{-}KO}$ mice
The staining of (A) Sirius red, (B) Masson blue, (C) COL1A1 and (D) αSMA in CCl_4-induced liver fibrosis. (n = 10, scale bar = 500 μM, * $p < 0.05$)

Consistent with histological results, there is significant protein elevation of collagen accumulation and HSC activation in the ablation of LSEC-specific HGF group (Figures 6A and B).

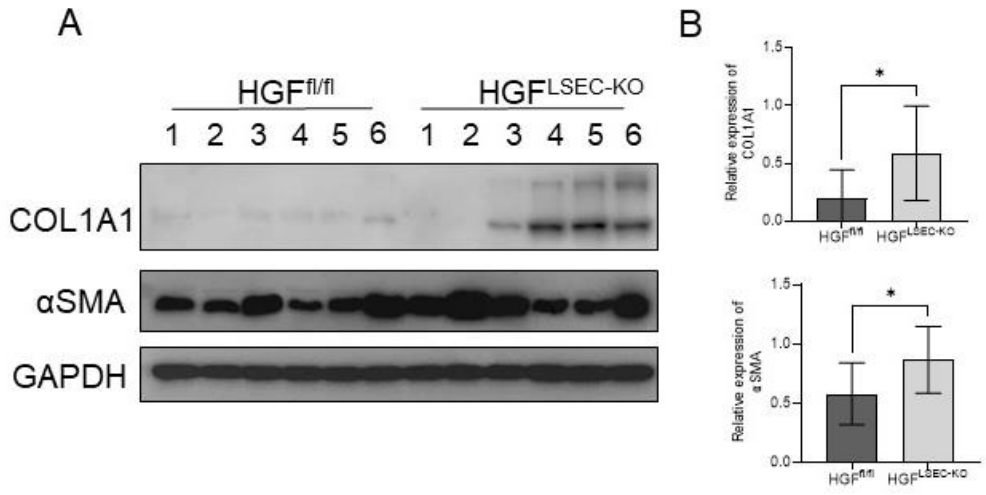

Figure 6. Collagen and HSC activation analysis after CCl_4-induced hepatic fibrosis in $HGF^{fl/fl}$ and $HGF^{LSEC\text{-}KO}$ mice
(A) Protein expression of COL1A1 in liver after CCl_4-induced liver fibrosis analysed by Western blot. (B) Quantification of each protein relative level in the representative samples. (n = 10, * $p < 0.05$).

4.3 Angiocrine HGF does not influence the immune microenvironment in liver fibrosis

It is reported that inflammation and fibrosis are associated inextricably in liver disease, whereby liver injury induces inflammation and the continuous liver inflammatory response facilitates liver fibrosis (Hernandez-Gea and Friedman 2011). Immune cells, especially liver-residing Kupffer cells and recruited macrophages, have been demonstrated as vital factors of liver inflammation that are essential to the progression or resolution of liver fibrosis (Koyama and Brenner 2017). On the other side, macrophage or neutrophil recruitment may participate in alleviating liver fibrosis (Rao, Wang et al. 2022). Persistence of the chronic liver injury during liver fibrosis may trigger the innate immune cells and activate pro-inflammatory cascade reactions (Del Campo, Gallego et al. 2018). Therefore, whether there is a link between inflammatory and angiocrine HGF, neutrophils, and macrophages in fibrotic liver of $HGF^{fl/fl}$ and $HGF^{LSEC\text{-}KO}$ mice was analysed. However, staining the markers of MPO and CD11b did

not reveal significant morphological changes of neutrophils and macrophages, respectively (Figures **7**A and B). Those helps to conclude that neutrophils and macrophages do not contribute to the influence of angiocrine HGF in the process of liver fibrosis.

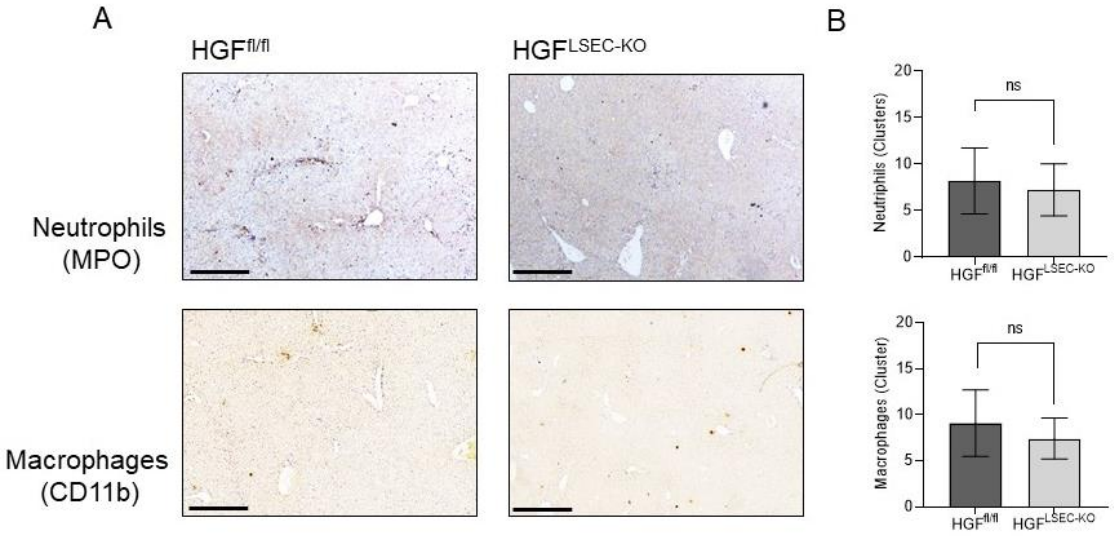

Figure 7. The deficiency of angiocrine HGF does not impact liver immune cell infiltration
(A) Representative MPO and CD11b staining of $HGF^{fl/fl}$ and $HGF^{LSEC\text{-}KO}$ mice in CCl_4-induced liver fibrosis. (B) Quantification of positive staining of MPO and CD11b in liver tissue. scale bar = 500 μM. (ns = no significance)

4.4 Angiocrine HGF mitigate the activation of HSCs in liver fibrosis

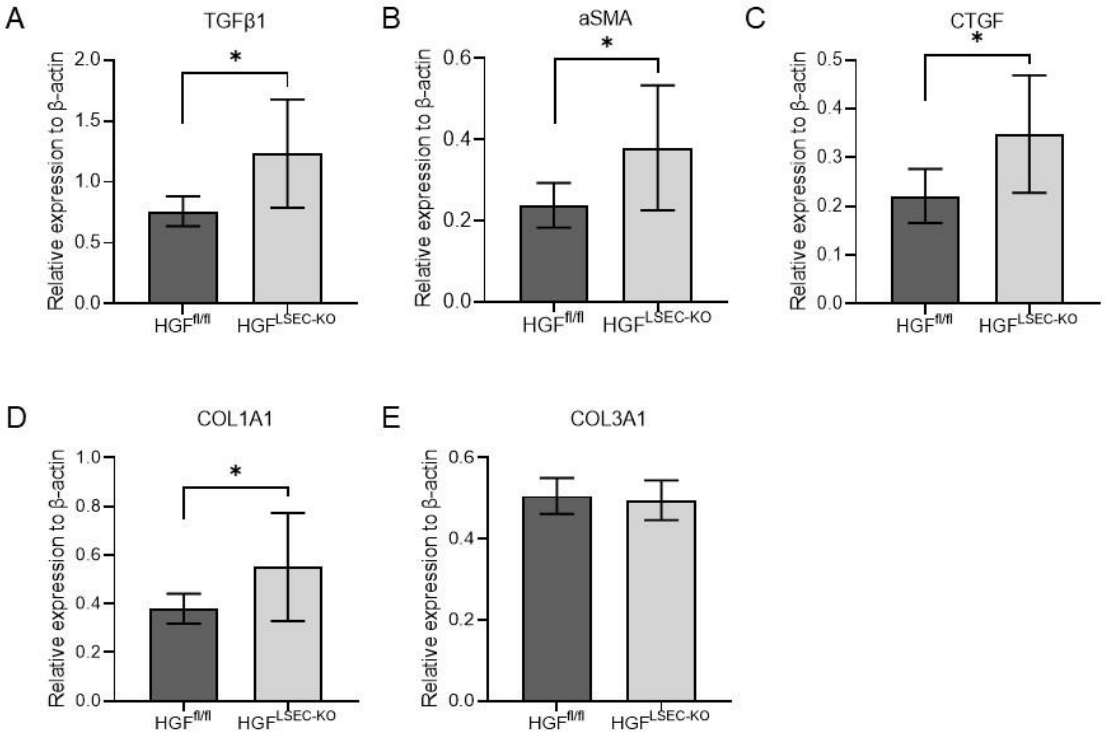

Figure 8. Collagen accumulation and HSC activation in isolated HSCs
Relative mRNA expression of (A) TGFβ1, (B) αSMA, (C) CTGF, (D) COL1A1, and (E) COL3A1. (ns = no significance, * $p < 0.05$)

HSCs are activated and contribute to the collage production consequentially following chronic injury. We selected the well-established isolation protocol for HSCs (Grunwald, Harant et al. 2016). HSCs may be transdifferentiated to myofibroblasts, producing the main parts of ECM, which include collagen and aSMA as shown in Figure 2. Furthermore, transforming growth factor (TGFβ1) secreted by activated HSCs could initiate a feedback, activating quiescent HSCs, to positively accelerate fibrogenesis (Li, Deng et al. 2021). In this study, after knockout of the expression of HGF in LSECs, it was found that, besides aSMA, TGFβ1, and COL1A1, connective tissue growth factor

(CTGF) is also elevated in the $HGF^{LSEC-KO}$ mice (Figures 8A, B, C and D). This is also considered as an important fibrotic mediator in this pathological process (Makino, Hikita et al. 2018). But there is no difference in the mRNA level of COL3A1 (Figure 8E).

Meanwhile, regarding the degradation and deposition of ECM, tissue inhibitor of metalloproteinase (TIMP)-1 and TIMP2 also serve as signs of HSC activation. Among the TIMPs, TIMP1 is a pivotal one, initiating MMP inhibition and the following ECM accumulation. TIMP2 could inapparently increase and inhibit the level of MMP2 (Hemmann, Graf et al. 2007). Moreover, TIMP1 and TIMP2 are mainly provoked from HSCs in the CCl_4 and bile duct ligation model (Herbst, Frey et al. 1997; Iredale 1997; Roeb, Purucke et al. 1997). Herein, it was found that TIMP1 shows an elevated level in the $HGF^{LSEC-KO}$ mice, indicating this may participate in the function of HGF in attenuating liver fibrogenesis. Vimentin is another marker elevated in liver fibrosis and most mesenchymal cells express vimentin, which maintains the structure of the cytoskeleton (Wang, Wu et al. 2019), though vimentin does not show any significant difference related to angiocrine HGF.

Next, in the presence of severe fibrosis, MMP1 is increased in the liver (Hemmann, Graf et al. 2007) and inhibited by TGFβ (Overall, Wrana et al. 1989). MMP2 is another factor increased with the fibrosis process and TIMP1 is able to inhibit the protein level of MMP2 (Iredale 1997; Iredale, Benyon et al. 1996). The upregulation of MMP9 has been confirmed both in protein and mRNA levels in the early weeks of recovery from fibrosis, and may indirectly contribute to HSC apoptosis (Hemmann, Graf et al. 2007). At present, we first focused on the role of TIMPs and MMPs in the pathological process of liver fibrosis in the different background of angiocrine HGF. Intriguingly, only TIMP1 and MMP2 were statistically elevated in the $HGF^{LSEC-KO}$ mice (Figures 9A and

E), which is consistent with the severity of liver fibrosis. Whereas vimentin, TIMP2, MMP1, and MMP9 do not show any differences in $HGF^{LSEC\text{-}KO}$ mice compared to the WT group (Figures 9B, C, D, and F).

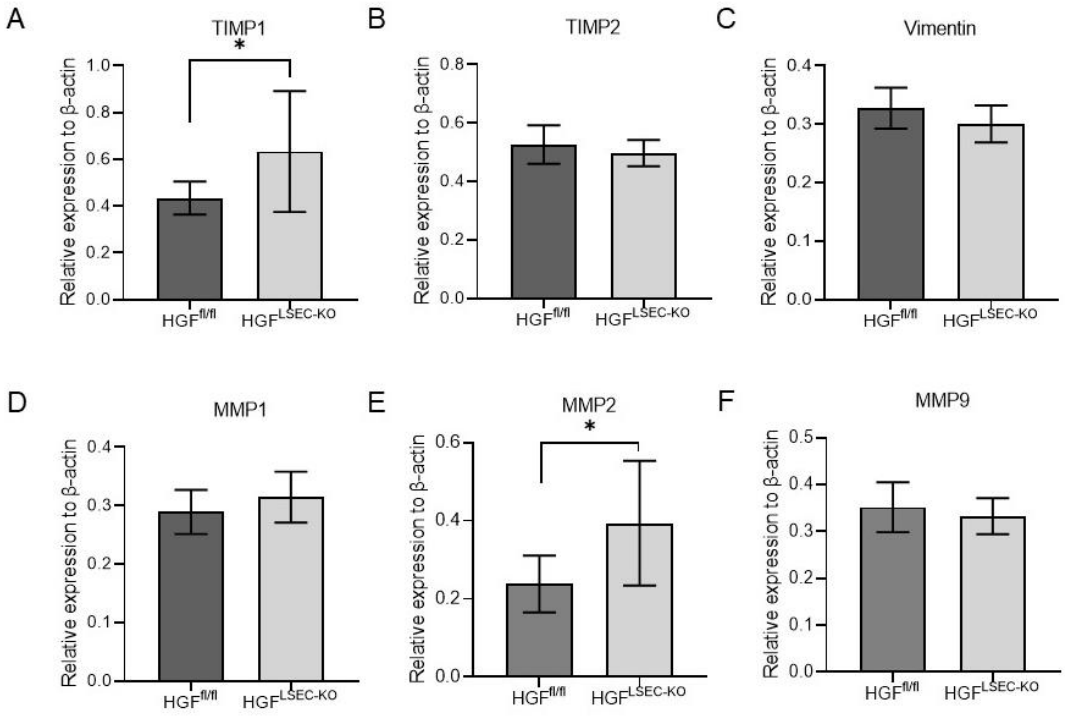

Figure 9. The alteration of metalloproteinases and tissue inhibitors of metalloproteinases impacted by angiocrine HGF

Relative mRNA expression of (A) TIMP1, (B) TIMP2, (C) Vimentin, (D) MMP1, (E) MMP2 and (F) MMP9 in $HGF^{fl/fl}$ and $HGF^{LSEC\text{-}KO}$ mice. (ns = no significance, * $p < 0.05$)

4.5 The status of LSECs capillarisation is altered in HGF$^{LSEC-KO}$ mice with liver fibrosis

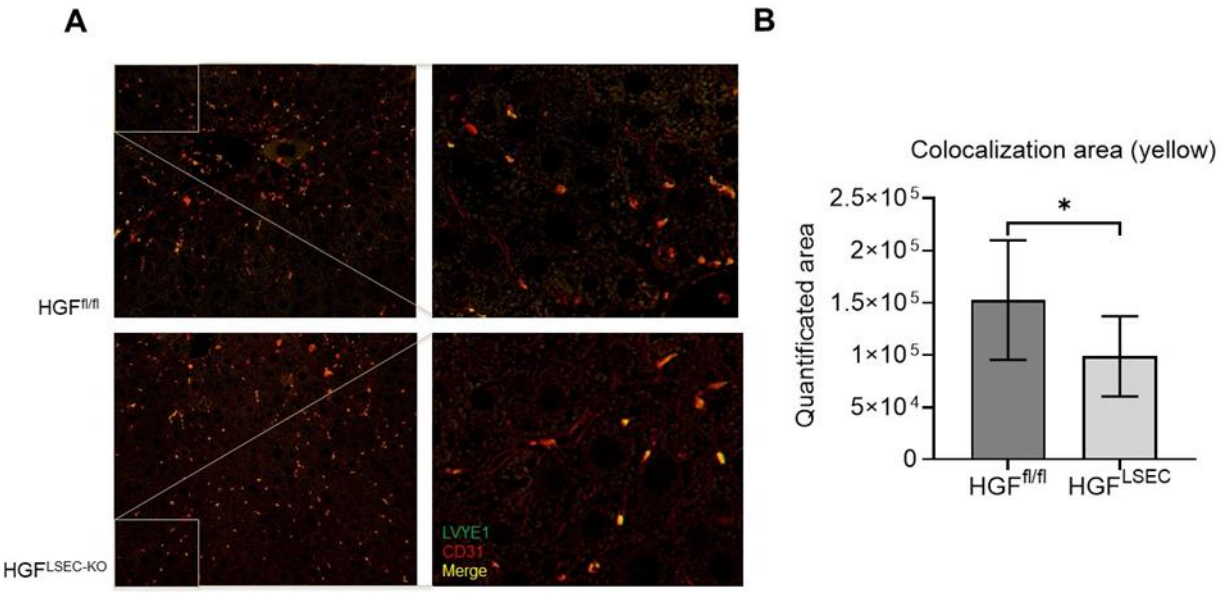

Figure 10. Angiocrine HGF alters capillarisation of LSECs in liver fibrosis
(A) Representative IF staining of LYVE1 and CD31 in liver tissue and (B) quantification of the colocalised positive area in control and HGF$^{LSEC-KO}$ mice. (* $p < 0.05$)

It was reported that the reversal of capillarised LSECs prevent the ongoing progression of fibrosis and the activation of HSCs (Xie, Wang et al. 2012). LYVE1 was demonstrated as a terminal differentiation marker of LSECs (Geraud, Koch et al. 2017), whereas CD31 was regarded as a marker of capillarisation and was highly expressed in vascular endothelial cells (Su, Yang et al. 2021). In patients at any degree of chronic active hepatitis or in laboratory liver fibrotic models, the capillarisation of hepatic sinusoidal endothelial cells precedes the occurrence of hepatic fibrosis (Bardadin and Desmet 1985; DeLeve, Wang et al. 2008b; Pasarin, La Mura et al. 2012). This indicates that the capillary vascularisation of hepatic sinusoidal endothelial cells may trigger liver fibrosis. Co-immunofluorescence (CO-IF) of LYVE1 and CD31 was used to evaluate the capillarisation of LSECs in the current study (Figures 10A and B). Quantification of

colocalisation analysis of LYVE1 and CD31 with ImageJ revealed the obvious reduction of the colocalisation area in the $HGF^{LSEC\text{-}KO}$ group. Thus, it can be concluded that angiocrine HGF increases the capillarisation level of LSECs.

4.6 Angiocrine HGF is negatively correlated with the severity of liver fibrosis in patients

To further verify the role of angiocrine HGF in patients, we collected liver tissues from 10 patients with surgical hepatectomy. VE-cadherin (also known as cadherin-5, CD144) locates in EC junctions and is regarded as an endothelial marker (Schrage, Loddenkemper et al. 2008; Su, Yang et al. 2021). As a major determinant of endothelial cell contact integrity, VE-cadherin is implicated in EC processes in the vascular development and in controlling the permeability of the vessel wall to cells and substances (Claesson-Welsh, Dejana et al. 2021). Nevertheless, fluorescence in situ hybridisation (FISH) of both HGF (Cy3) and VE-cadherin proteins shows the expression of HGF and the morphology of LSEC (Figure 11A). Combined with fibrosis score, HGF levels in LSECs in all of the patients with chronic liver injury were negatively correlated with the severity of fibrosis (Figure 11B), which is consistent with our results in the mouse model. Taken together, the above results suggest that the level of HGF in LSECs can be used as a potential target for clinical treatment of patients with chronic liver fibrosis.

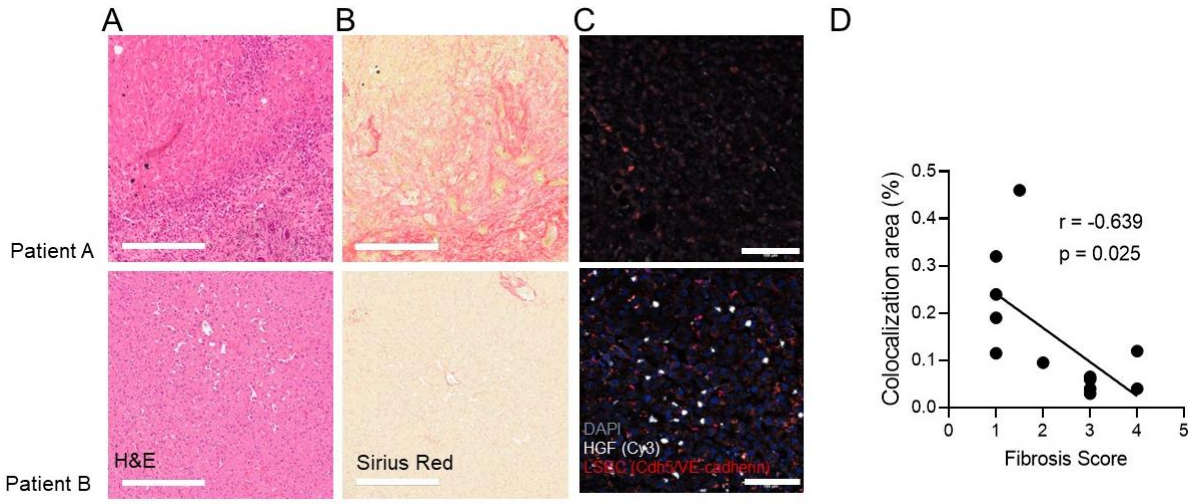

Figure 11. Correlation of angiocrine HGF and hepatic fibrosis in patients
Representative images of the patients with higher- (patient A) and lower- fibrosis score (patient B) stained with (A) H&E, (B) Sirius red (bar = 300 μM) and (C) FISH for Cy3 and Cdh5/VE-cadherin (bar = 100 μM) in the fibrotic liver tissues from surgical hepatectomy patients (n = 10). (D) value in liver tissue. Pearson correlation analysis between HGF in LSECs and fibrosis score and the quantification of HGF (white) and LSEC (red) protein level, which is represented in integrated optical density (IOD).

4.7 Ablation of HGF in LSECs activates the PDK1/Akt axis in CCl_4-induced liver fibrosis

3-Phosphoinositide-dependent kinase 1 (PDK1) is a molecular kinase involved in the phosphoinositide-3-kinase (PI3K) signalling pathway, which acts as a major molecule participating in a variety of cellular functions. It has been demonstrated that Akt may facilitate PDK1-dependent phosphorylation of Akt, and the activation of Akt regulates many downstream targets (Fyffe and Falasca 2013). Meanwhile, the PDK1/Akt axis was reported as associated with fibrosis (Jia, Agarwal et al. 2018), and HGF regulates the PI3K/PDK/Akt signal by initiating the G protein-coupled receptor, which contributes to cell growth and cell protection (Okano, Shiota et al. 2003). Therefore, investigation of the most correlated signalling pathway may implicate the regulation of angiocrine HGF in liver fibrogenesis. The levels of Akt present a similar tendency in all the mice livers (Figure 12A and B). However, comparison of $HGF^{fl/fl}$ and $HGF^{LSEC\text{-}KO}$ mice revealed a significant increase in phosphorylated Akt and phosphorylated PDK1 in

the ablation of HGF in LSECs. These results indicate the impaired role of angiocrine HGF in the PDK1/Akt axis after fibrosis.

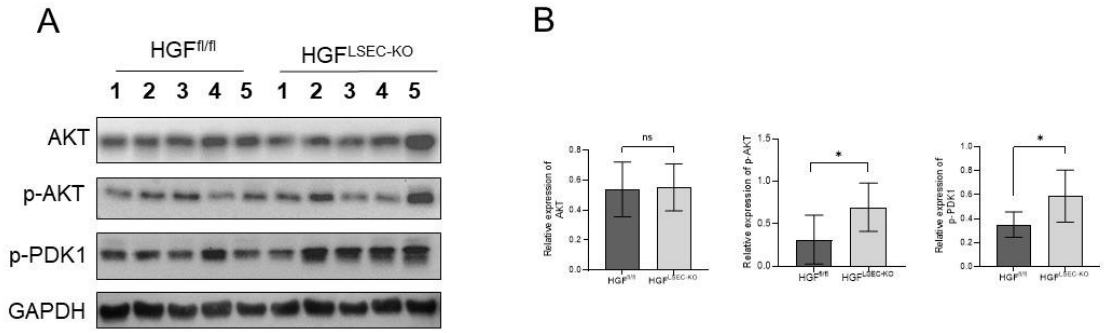

Figure 12. Deletion of HGF in LSEC increases p-Akt expression and the downstream regulators in CCl_4-induced liver fibrosis
(A) Representative western blots and (B) quantification of Akt, phosphorated-Akt, phosphrated-PDK1 in fibrotic livers from $HGF^{fl/fl}$ and $HGF^{LSEC-KO}$ mice. Results are normalised to GAPDH. (mean ± S.D., ns = no significance, * $p < 0.05$)

4.8 Angiocrine HGF attenuates collagen formation and activation of HSCs *in vitro*

Transforming growth factor (TGF)-β, derived from various cellular type such as HSCs, LSECs, platelets, macrophages, and hepatocytes, is activated in the ECM deposits during chronic hepatic injury. TGFβ then induces HSC activation and ECM deposition by binding TGF-β type II receptor (TβRII), phosphorylates the downstream substrates, and thereafter regulates target genes such as connective tissue growth factor (CTGF) and αSMA (Dewidar, Meyer et al. 2019). Besides, it primarily establishes the mechanism of angiocrine HGF in the process of liver fibrosis *in vivo* and clinic patients (De Angelis Rigotti, Wiedmann et al. 2023). Additionally, HS-173, the inhibitor of the PI3K/Akt signalling pathway, verified both *in vitro* and *in vivo*, exhibited a suppressed function in liver fibrotic responses, including obviously

suppressed phosphorylation of Akt, and decreased expression of collagen I, TIMP-1, and MMP-2 in CCl_4-related hepatic fibrosis (Son, Ryu et al. 2013). Therefore, integrated with our findings, the isolated HSCs were subdivided to four groups, including untreated, TGF-β stimulation (10 ng/mL), TGF-β (10 ng/mL) and HGF (10 ng/mL), and HS-173 (50 mM), to verify the potential relationship between angiocrine HGF and Akt-related mechanisms. CTGF and COL1A1 (Figures 13A and B) were consistent with the results of the *in vivo* experiment (Figures 8C and D). HGF could mitigate the TGFβ-stimulated activation of HSC. Nevertheless, there is no effect of HGF on TIMP1 and MMP2 (Figures 13C and D), and the activation of Akt contributes to TIMP1 and MMP2 *in vitro* (Figures 13E and F). There is an intriguing correlation of Akt pathway participation in angiocrine HGF *in vivo* (Figures 9A and E) but not *in vitro* (Figures 13E and F).

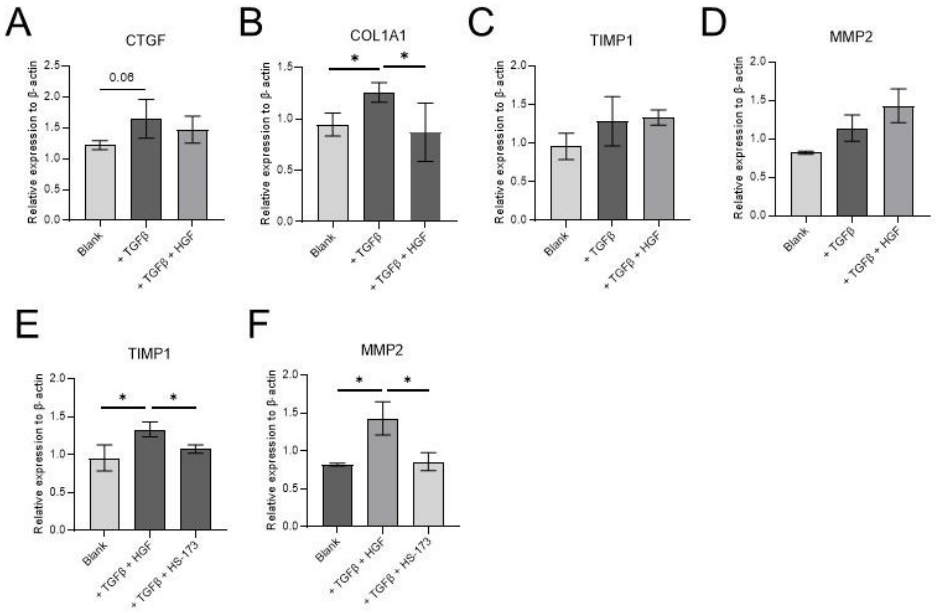

Figure 13. The role of recombinant HGF for the *in vitro* HSCs
Relative mRNA expression of (A) CTGF, (B) COL1A1, (C) TIMP1, (D) MMP2, (E) TIMP1, and (F) MMP2. Three replications for each group. (mean ± S.D., * $p < 0.05$, ** $p < 0.01$)

4.9 Aquaporin 4 is downregulated by angiocrine HGF in liver fibrosis

Finally, to best investigate the regulatory pathway of angiocrine HGF in pathological liver fibrosis in the mice, RNA sequencing was applied to whole liver RNA from untreated and 4-week CCl_4 injected mice, post-liver fibrosis. Based on the raw generated RNA sequencing FPKM data matrix, limma package was performed to identify the angiocrine-related altered factors among the groups. Aquaporin 4 (AQP4) was found to be the most upregulated gene in the mice where HGF is ablated in LSEC (Figures 14A and B). AQP4 functions as a water channel protein and is demonstrated as an essential factor in brain-water regulation in a hepatic encephalopathy (Dhanda and Sandhir 2018; Rama Rao, Verkman et al. 2014). However, AQP4 could affect the abnormalities of collecting duct water transport in chronic common bile duct ligation (Fernández-Llama, Turner et al. 1999), though it has not been well investigated in liver fibrosis.

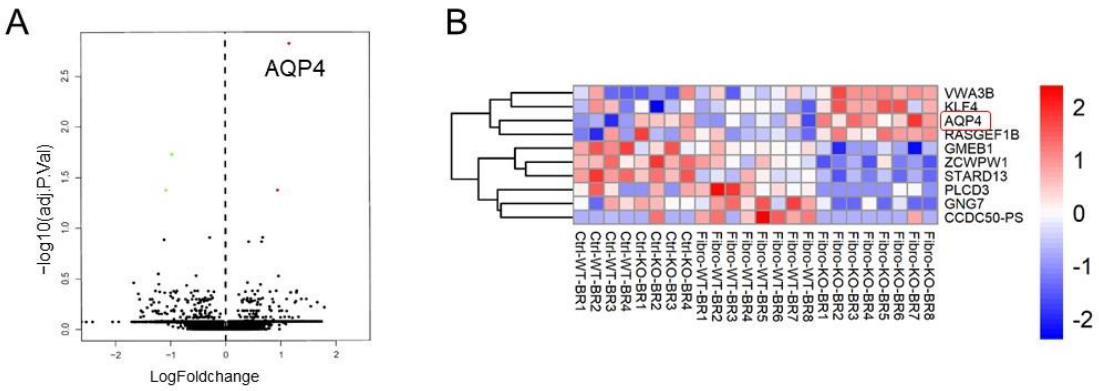

Figure 14. Identification of key regulators by RNA-seq
(A) Volcano plot and (B) heatmap of RNA-seq in the enrolled untreated and CCl_4-injected mice. Blue colour refers to downregulated genes and red colour refers to upregulated genes in the liver sample. The colour scale means z-scaled gene expression level.

To further verify the protein level of the RNA sequencing results,

immunohistochemistry staining was implicated for AQP4 and found it was significantly increased in the $HGF^{LSEC-KO}$ mice compared to WT mice in fibrotic liver tissue (Figures 15A and B). Therefore, AQP4 is upregulated in $HGF^{LSEC-KO}$ mice, which provides a clue that AQP4 may be involved in the regulation of HGF.

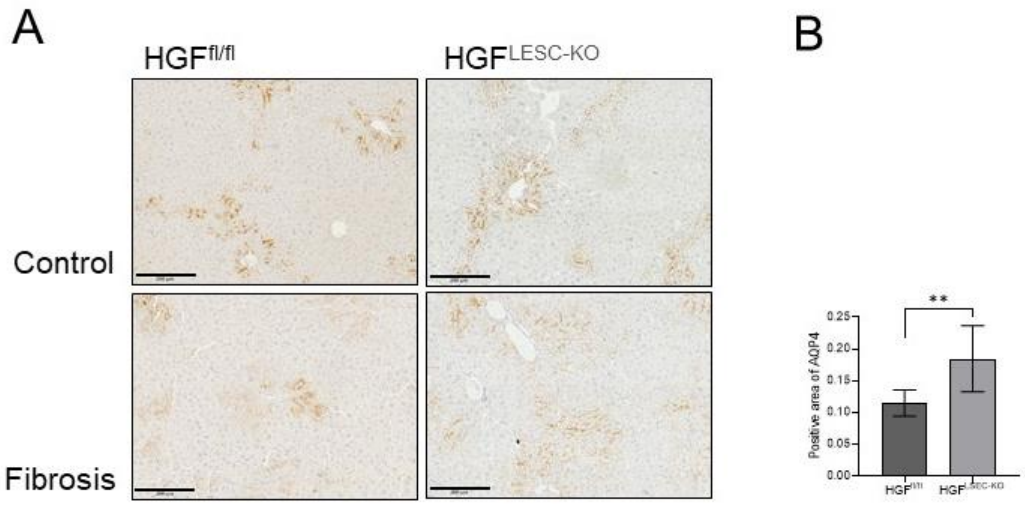

Figure 15. Verification of AQP4 in control and fibrotic liver tissue
(A) Representative immunohistochemistry staining of AQP4 and (B) quantification of positive area from fibrotic liver tissues of $HGF^{fl/fl}$ and $HGF^{LSEC-KO}$ mice. (n = 10, scale bar = 200 μM, results are represented as mean ± S.D., ** $p < 0.01$)

5 DISCUSSION

5.1 LSEC-specific HGF knockout mice model and liver fibrosis

LSECs, like the other ECs, express CD31 (PECAM) but CD31 is restricted to the cytoplasm in normal LSECs (DeLeve, Wang et al. 2004). As a kind of specialised capillary ECs of the liver to deliver blood, they are essential for liver metabolism and fibrosis (DeLeve 2013; Leibing, Geraud et al. 2018; McConnell, Kostallari et al. 2023; Rafii, Butler et al. 2016). Despite that HGF is critical in liver growth and essential in the protective role of injured liver or other organs (Nakamura and Mizuno 2010), there is still an unmet demand to reveal the specific role of angiocrine HGF in liver fibrosis. For animal research, there are many kinds of methods that were used to proceed with the research. For example, notch activation in LSECs, reducing the HGF and other critical hepatocyte mitogens and enhancing the fibrotic level induced by CCl_4 (Duan, Ruan et al. 2018). Meanwhile, tamoxifen-caused EC-specific deletion of HGF does not lead to pathological alteration in metabolic or liver development (Cao, Ye et al. 2017). Besides, though it was previously demonstrated that the inducible EC-derived HGF can mitigate transplanted parenchymal reconstitution in acute injured mouse liver (Cao, Ye et al. 2017), the inducible EC-specific knockout mouse model is a transient deprivation of angiokines, and the constitutive ablation of the HGF model is better to investigate fibrogenesis in long-term development.

Cre-loxP-mediated conditionally genetic modification technology has been well established in LSEC-specific knockout mice. For example, incomplete stab2-icre-driven GATA4 deficiency in LSECs causes perisinusoidal liver fibrosis (Winkler, Staniczek et al. 2021). Here, we got the conditional HGF deletion in LSECs by crossing stab2-icre

with $HGF^{fl/fl}$ mice. And our previous study revealed a reduced organismal growth but healthy liver development in such an endothelial-selective HGF deficiency (Zhang, Olsavszky et al. 2020). In the current study, a lower liver to body ratio in normal $HGF^{LSEC\text{-}KO}$ mice was found, even though there is no statistical significance. Similarly, the histological study also did not reveal any obvious inflammation, or morphological changes according to H&E, Sirius red, and serum test for liver functions. Collectively, $HGF^{LSEC\text{-}KO}$ mice embrace healthier liver development and function.

5.2 The deletion of HGF in LSECs enhances liver fibrosis at the early stage of hepatic fibrosis

HSCs are one of the components of liver non-parenchymal cells, and they activate in the occurrence and development of liver fibrosis. HSCs can synthesise ECM, regulate sinusoidal blood flow. and synthesise metalloproteinases. In the setting of liver damage after various stimulators, HSCs differentiate to trans-smooth muscle alpha-actin containing myofibroblasts and generate related inflammatory cytokines (Hazrati, Malekpour et al. 2022). Recently, numerous mechanisms of hepatic fibrosis were investigated and remarkable progress has been made in elucidating the pathophysiology of liver fibrosis, but there is still an unmet demand to discover new therapeutic targets. CCl_4-induced mouse hepatic fibrosis was used in this study since the CCl_4 could induce persistent liver damage, inflammation, and HSCs activation (Dong, Chen et al. 2016), and the pathogenesis of fibrosis is closely associated to proliferation of connective tissue (Guo, Xu et al. 2013). There are many reports focused on HGF in the liver, though its specific role derived from LSECs in liver fibrosis remains unknown. For example, HGF could promote cell survival, liver regeneration, and alleviate chronic inflammation (Jangphattananont, Sato et al. 2019; Michalopoulos and Khan 2005).

Here, focused on a dynamic period of CCl_4-induced liver fibrosis, we found there is no difference in fibrotic level between the $HGF^{fl/fl}$ and $HGF^{LSEC\text{-}KO}$ groups after 6 or 8 weeks of CCl_4 injection. However, it presented a statistically significant phenotype after 4 weeks of CCl_4 injection in the $HGF^{LSEC\text{-}KO}$ mouse compared to the $HGF^{fl/fl}$ group. It may cause other signals that compensate for the mitogenic function of LSEC-specific HGF ablation if exposed to a long period of liver injury, which needs to be investigated in the future. It is previously reported that the liver/body weight ratio was decreased, and AST and ALT were both elevated significantly in CCl_4-treated group (Dong, Chen et al. 2016). And a similar result in $HGF^{LSEC\text{-}KO}$ mice treated with CCl_4 was found, which presented with a lower liver/body weight ratio and higher liver damage level. Meanwhile, staining like Sirius red, Masson blue, and COL1A1, as well as α-SMA, showed angiocrine HGF attenuates collagen deposition and HSC activation. All these results suggest angiocrine HGF can alleviate the pro-fibrotic response and suppress the progression of liver fibrogenesis. Here, for the first time, we conclude that the ablation of HGF in LSECs fundamentally promote fibrotic progression in the early stages after CCl_4 injection, but not in long-term fibrosis (extended to 6 or 8 weeks).

Additionally, immune system cells, such as KCs, circulating macrophages, or neutrophils, are key cells for the activation of TGF-β1-mediated HSCs and then promote their NF-κB-dependent survival probabilities in liver fibrogenesis (Gandhi 2017; Hazrati, Malekpour et al. 2022). But our results indicate that angiocrine HGF does not influence immune cell infiltration in CCl_4-induced liver fibrosis, indicating the potential mechanism of angiocrine may lay on other signalling pathways.

Besides, in the process of hepatic fibrosis, LSECs transferred the phenotype to proceed with fibrosis, otherwise called capillarisation. In the rat model, it was found that the

reversal of capillarised LSECs prevented the progression of fibrosis (Xie, Wang et al. 2012), whereby this type of LSEC loses the function to mitigate activated HSCs. The active endothelial cells can be protective in liver parenchymal inflammation in the initiation of perisinusoidal fibrosis by prohibiting noxious agents from the blood into liver parenchyma (Bardadin and Desmet 1985). In patients at any degree of chronic active hepatitis or in laboratory fibrotic models, the capillarisation of hepatic sinusoidal endothelial cells precedes the occurrence of hepatic fibrosis (Bardadin and Desmet 1985; DeLeve, Wang et al. 2008b; Pasarin, La Mura et al. 2012). In the situation of persistent liver damage—chronic inflammation—LSECs lose the function and get involved in the onset and progression of the whole liver disease, including sinus capillary formation, angiogenesis, alteration of angiocrine signals, and reconstruction of vessels (Cogger, Arias et al. 2008). Nevertheless, differentiated LSECs contribute to the maintain quiescent HSCs in former experimental *in vivo* models (Deleve, Wang et al. 2008a), and restoration of differentiated LSECs alleviates regression of mild fibrosis (Xie, Wang et al. 2012). In this study, by applying the CO-IF staining of LYVE1 and CD31 on the established mouse fibrosis model, we found that angiocrine HGF attenuates the status of LESCs capillarisation. This suggests that the capillary vascularisation of hepatic sinusoidal endothelial cells participated in triggering liver fibrosis.

In conclusion, the pathological remodelling of hepatic sinusoids plays an important role in the occurrence and development of hepatic fibrosis. Capillary vascularisation of hepatic sinusoidal endothelial cells not only mediates the microenvironment of hepatic fibrosis, but also promotes the activation of HSCs and promotes the progression of hepatic fibrosis. At present, our understanding of hepatic sinusoidal endothelial cell

capillarisation remains to be further elucidated.

5.3 The role of angiocrine HGF in patients with liver fibrosis

Though the genetically altered animal model is the currently accepted method for deciphering the specific gene function *in vivo*, compensatory mechanisms are still possible in adult liver tissue development. The staining analysis of some liver biopsies of fibrotic liver tissue from patients with hepatitis C revealed that capillarisation of LSECs persists even with the regression of fibrosis (D'Ambrosio, Aghemo et al. 2012). And the source of HGF is mostly derived from LSECs, especially in the setting of liver injury (DeLeve 2013; Poisson, Lemoinne et al. 2017). As attested by the mutual therapeutic effects of these two pathological processes, hepatic fibrosis promotes angiogenesis while angiogenesis aggravates fibrosis in turn (Taura, De Minicis et al. 2008; Thabut, Routray et al. 2011). Noteworthy, in chronic liver disease, the therapeutic drug strategies targeting LSECs, such as statins, can improve liver fibrosis and portal hypertension (Abraldes, Albillos et al. 2009; Abraldes, Villanueva et al. 2016; Marrone, Russo et al. 2013). Indeed, the exact mechanism of HGF derived from LSECs in the mild stage of hepatic fibrosis in patients remains unknown. There are no unique markers for LSECs identification, though some markers, including CD31 or CD144 (VE-cadherin), are being discussed as to delineate the location of LSECs in liver tissue (Geraud, Koch et al. 2017; Poisson, Lemoinne et al. 2017). In the present study, we applied combined HGF with VE-cadherin for locating HGF in LSECs in patient liver tissue, which is the first to reveal the negative correlation between specific angiocrine HGF and fibrotic level in a dynamic development of liver fibrosis.

5.4 The deletion of HGF in LSECs impacts the PDK1/Akt axis in hepatic fibrosis

3’phosphoinositide-dependent protein kinase-1 (PDK1) is an upstream kinase for the activation of Akt. It was previously demonstrated that HGF-elicited migration of mesenchymal stem cells (MSCs) was associated with the downstream activation of PDK1 and Akt (He, Wang et al. 2018). Previous studies report that the activation of PDK1/Akt signalling can be triggered by some growth factors and some ECM (Dimmeler and Zeiher 2000; Lamalice, Le Boeuf et al. 2007), having a pro-fibrotic role in various organ fibrosis (Paik, Kim et al. 2009). Phosphorylated PDK1 increases the activation of Akt and subsequently reduces the phosphorylation of GSK3β (Han, Wang et al. 2022). PDK1/Akt signalling activates the downstream PI3K expression, which is important for various cellular functions such as fibroblasts and endothelial cells (Gagliardi, Puliafito et al. 2018). Additionally, PDK1-induced phosphorylation of Akt in endothelial cells is necessary for angiogenesis (Park, Lee et al. 2015). HGF, depending on the PDK1/Akt pathway, can alleviate the inflammatory response in renal injury, as well (Gui and Dai 2020). However, previous studies on the cellular function of HGF have mainly focused on the parenchymal cells in various organs, and the mechanism of HGF in mesenchymal cells is rarely reported. In this study, we focused on the PDK1/Akt pathway and first revealed the potential relationship of angiocrine HGF to mitigate phosphorylated PDK1 and thus decrease the activation of Akt to alleviate liver fibrotic severity.

5.5 Angiocrine HGF impacts the balance of MMPs/TIMPs in liver fibrosis

Furthermore, regardless of the causes, HSCs increase in early fibrosis and regulate with the severity of fibrosis (Jindal, Jagdish et al. 2022), and normal LSECs can prevent HSC activation and inactivate the activated HSCs (Deleve, Wang et al. 2008a). Pro-HGF is released from ECM, whereas MMPs can degrade ECM (Fujiyoshi and Ozaki 2011). Signals of persistent liver injury and inflammation are synthesis of ECM components and the imbalance of MMPs/TIMPs (Zhang, Hua et al. 2022). MMPs are critical for a variety of inflammatory diseases and mediate the "turnover" effect of the remodelling process of ECM. Some MMPs play an anti-fibrotic role but others have the opposite effect, among them, MMP2 and MMP9 are primarily produced to increase fibrogenesis but not fibrolysis (Robert, Gicquel et al. 2016). Additionally, the synthesis and function of MMPs are regulated not only by the transcriptional activation, but also the tissue inhibitors of metalloproteinases (TIMP1) (Robert, Gicquel et al. 2016). It is reported that TIMP1 is significantly correlated with the severity of liver fibrosis (Yata, Takahara et al. 1999), whose production may be caused by Kupffer cells and hepatocytes in the early stages of liver damage, and is demonstrated in other animal experiments (Bergheim, Guo et al. 2006; Iredale, Benyon et al. 1996; Kossakowska, Edwards et al. 1998). Though TIMP1 itself does not cause the fibrosis (Yoshiji, Kuriyama et al. 2000; Yoshiji, Kuriyama et al. 2002), a previous study revealed that TIMP-1 can not only increase MMP activity, but also serve as a negative regulator of HGF, which impacts HGF bioactivity and therefore shifts the cell cycle during hepatic regeneration (Mohammed, Pennington et al. 2005). Additionally, TIMP1 can induce the activation of PI3K and the subsequent PDK1 by binding to CD63 and β1 integrin in

melanoma (Toricelli, Melo et al. 2017), which provides a clue to the association between TIMP1 and PDK1. Besides, TIMP/MMP axis is a novel upstream of HGF signalling during liver regeneration and fibrosis (Mohammed, Pennington et al. 2005), acting as a preventor in the activation of HSC and the subsequent MMPs and collagen synthetisations (Han, Zhou et al. 2004). In the present study, when the HGF is ablated in LSECs, it was found that the level of MMP2 and TIMP1 were elevated after CCl_4 induction in the whole liver. It was reported that Pien-Tze-Huang alleviates the level of MMP2, MMP9, and TIMP1 in CCl_4-induced live fibrosis (Zhang, Hua et al. 2022). And MMP1 were negatively associated with the severity of fibrosis but TIMP1 embraces the opposite function (Grunwald, Schoeps et al. 2019). MMPs such as MMP1, MMP2, and MMP9 are known to process collagens in fibrogenesis (Shan, Wang et al. 2023), but no obvious changes were found in MMP1 and MMP9. Taken together, we show that angiocrine HGF, in turn, affects the upstream TIMP1 and MMP2 expression during hepatic fibrosis.

As to the *in vitro* experiment, TGFβ1 can promote activity of MMP2, which conversely suppresses collagen type I expression. Besides, MMP2, as well as TIMPs in fibrotic tissue, were increased by α-SMA-positive myofibroblast-like cells (Roeb 2018). Additionally, HS-173, the inhibitor of the PI3K/Akt signalling pathway, can suppress Akt activation, decrease expression of collagen I, TIMP-1, and MMP-2 in CCl_4-related hepatic fibrosis (Son, Ryu et al. 2013). HS-173 also improves stability of endothelial vessel structure and vascular maturity, as well as notch signalling in ECs (Kim, Jung et al. 2017). As to the results shown in this study, by using TGFβ1 on HSC *in vitro*, the different roles of HGF for TIMP1 and MMP2 were found in the cell experiments when compared to the in vivo results, indicating the changes of other mechanisms, such as

notch signalling in LSECs, may serve as a factor that makes the difference between *in vitro* and *in vivo* findings. These need to be further verified in the future. Integrated with the current study, however, it shed light on the mutual tuning of HGF and TIMP1 in liver fibrosis.

5.6 AQP4 is downregulated by angiocrine HGF during liver fibrosis

By RNA-seq, we screened the most significant gene, AQP4, which is remarkably elevated in the $HGF^{LSEC\text{-}KO}$ mouse liver fibrosis model. Given there is little research reporting on the role of AQP4 participation in liver fibrogenesis, the activation of the PDK/Akt pathway can weaken the following AQP4 expression, which consequently reduces brain oedema, Alzheimer's disease, and acute lung injury (Chen, Deng et al. 2020; Guo, Wu et al. 2019). Concurrently, Glycyl-l-histidyl-l-lysine (GHK) alleviates the inflammatory reaction in intracerebral haemorrhage by upregulating the expression of AQP4, and the activation of the PDK/Akt pathway, and also relieved the MMP2, synchronously (Zhang, Wang et al. 2020). Here, we performed verification experiments to confirm the protein level of AQP4 both in mouse and human tissues. The higher severity of fibrosis caused by the deficiency of HGF generated by LSECs may be associated with the level of AQP4. To this end, this topic firstly used bioinformatics analysis as the breakthrough point to find the relationship between HGF expression and different clinical liver disease stages, and to observe the role of HGF protein through CCl_4-induced liver fibrosis in a transgenic mouse model.

6 SUMMARY

Facing the potential reversible status of liver fibrosis, it is an effective method to elucidate the pathological development and thus help to terminate the progression to cirrhosis, liver failure, or HCC. In the present study, the new fibrotic model of LSEC-specific HGF knockout mice ($HGF^{LSEC\text{-}KO}$) was used to comprehensively investigate mechanisms during liver fibrogenesis. In fibrotic liver tissue, $HGF^{LSEC\text{-}KO}$ expressed more severe liver damage, HSC activation, and liver fibrosis, but not immune infiltration at the early stage upon CCl_4 administration. Meanwhile, it presents the same HSC activation and collagen accumulation in primary isolated HSCs. The ablation of HGF in LSECs can also reduce the capillarisation status of LSECs. In the fibrotic liver, the PDK1/Akt axis is mostly influenced by the deletion of LSEC-specific HGF. In addition, there is a negative correlation between LSEC-specific HGF and fibrotic level in clinic patients with fibrotic liver. Furthermore, AQP4 was screened as the most regulated gene in the deficiency of angiocrine HGF by RNA-seq and statistical analysis. Taken together, angiocrine HGF and the related molecule could be regarded as targets in liver fibrosis treatment. All in all, it is expected that in-depth research on the interference and level alteration of angiocrine HGF and related signalling components may pave the way for anti-fibrotic therapy in liver disease.

7 REFERENCES

Abraldes, J.G., Albillos, A., Banares, R., Turnes, J., Gonzalez, R., Garcia-Pagan, J.C., and Bosch, J. (2009). "Simvastatin lowers portal pressure in patients with cirrhosis and portal hypertension: a randomized controlled trial." Gastroenterology **136**(5): 1651-1658.DOI: 10.1053/j.gastro.2009.01.043.

Abraldes, J.G., Rodriguez-Vilarrupla, A., Graupera, M., Zafra, C., Garcia-Caldero, H., Garcia-Pagan, J.C., and Bosch, J. (2007). "Simvastatin treatment improves liver sinusoidal endothelial dysfunction in CCl4 cirrhotic rats." J Hepatol **46**(6): 1040-1046.DOI: 10.1016/j.jhep.2007.01.020.

Abraldes, J.G., Villanueva, C., Aracil, C., Turnes, J., Hernandez-Guerra, M., Genesca, J., Rodriguez, M., Castellote, J., Garcia-Pagan, J.C., Torres, F., Calleja, J.L., Albillos, A., Bosch, J., and Group, B.S. (2016). "Addition of Simvastatin to Standard Therapy for the Prevention of Variceal Rebleeding Does Not Reduce Rebleeding but Increases Survival in Patients With Cirrhosis." Gastroenterology **150**(5): 1160-1170 e1163.DOI: 10.1053/j.gastro.2016.01.004.

Arii, S., and Imamura, M. (2000). "Physiological role of sinusoidal endothelial cells and Kupffer cells and their implication in the pathogenesis of liver injury." J Hepatobiliary Pancreat Surg **7**(1): 40-48.DOI: 10.1007/s005340050152.

Aydin, M.M., and Akcali, K.C. (2018). "Liver fibrosis." Turk J Gastroenterol **29**(1): 14-21.DOI: 10.5152/tjg.2018.17330.

Bao, Y.L., Wang, L., Pan, H.T., Zhang, T.R., Chen, Y.H., Xu, S.J., Mao, X.L., and Li, S.W. (2021). "Animal and Organoid Models of Liver Fibrosis." Front Physiol **12**: 666138.DOI: 10.3389/fphys.2021.666138.

Bardadin, K.A., and Desmet, V.J. (1985). "Ultrastructural observations on sinusoidal endothelial cells in chronic active hepatitis." Histopathology **9**(2): 171-181.DOI: 10.1111/j.1365-2559.1985.tb02433.x.

Bataller, R., and Brenner, D.A. (2005). "Liver fibrosis." J Clin Invest **115**(2): 209-218.DOI: 10.1172/jci200524282.

Bergheim, I., Guo, L., Davis, M.A., Duveau, I., and Arteel, G.E. (2006). "Critical role of plasminogen activator inhibitor-1 in cholestatic liver injury and fibrosis." J Pharmacol Exp Ther **316**(2): 592-600.DOI: 10.1124/jpet.105.095042.

Campana, L., and Iredale, J.P. (2017). "Regression of Liver Fibrosis." Semin Liver Dis **37**(1): 1-10.DOI: 10.1055/s-0036-1597816.

Cannito, S., Paternostro, C., Busletta, C., Bocca, C., Colombatto, S., Miglietta, A., Novo, E., and Parola, M. (2014). "Hypoxia, hypoxia-inducible factors and fibrogenesis in

chronic liver diseases." Histol Histopathol **29**(1): 33-44.DOI: 10.14670/HH-29.33.

Cao, Z., Ye, T., Sun, Y., Ji, G., Shido, K., Chen, Y., Luo, L., Na, F., Li, X., Huang, Z., Ko, J.L., Mittal, V., Qiao, L., Chen, C., Martinez, F.J., Rafii, S., and Ding, B.S. (2017). "Targeting the vascular and perivascular niches as a regenerative therapy for lung and liver fibrosis." Sci Transl Med **9**(405).DOI: 10.1126/scitranslmed.aai8710.

Chapouly, C., Guimbal, S., Hollier, P.L., and Renault, M.A. (2019). "Role of Hedgehog Signaling in Vasculature Development, Differentiation, and Maintenance." Int J Mol Sci **20**(12).DOI: 10.3390/ijms20123076.

Chen, X., Deng, S., Lei, Q., He, Q., Ren, Y., Zhang, Y., Nie, J., and Lu, W. (2020). "miR-7-5p Affects Brain Edema After Intracerebral Hemorrhage and Its Possible Mechanism." Front Cell Dev Biol **8**: 598020.DOI: 10.3389/fcell.2020.598020.

Claesson-Welsh, L., Dejana, E., and McDonald, D.M. (2021). "Permeability of the Endothelial Barrier: Identifying and Reconciling Controversies." Trends Mol Med **27**(4): 314-331.DOI: 10.1016/j.molmed.2020.11.006.

Cogger, V.C., Arias, I.M., Warren, A., McMahon, A.C., Kiss, D.L., Avery, V.M., and Le Couteur, D.G. (2008). "The response of fenestrations, actin, and caveolin-1 to vascular endothelial growth factor in SK Hep1 cells." Am J Physiol Gastrointest Liver Physiol **295**(1): G137-G145.DOI: 10.1152/ajpgi.00069.2008.

Cogger, V.C., Roessner, U., Warren, A., Fraser, R., and Le Couteur, D.G. (2013). "A Sieve-Raft Hypothesis for the regulation of endothelial fenestrations." Comput Struct Biotechnol J **8**: e201308003.DOI: 10.5936/csbj.201308003.

D'Ambrosio, R., Aghemo, A., Rumi, M.G., Ronchi, G., Donato, M.F., Paradis, V., Colombo, M., and Bedossa, P. (2012). "A morphometric and immunohistochemical study to assess the benefit of a sustained virological response in hepatitis C virus patients with cirrhosis." Hepatology **56**(2): 532-543.DOI: 10.1002/hep.25606.

De Angelis Rigotti, F., Wiedmann, L., Hubert, M.O., Vacca, M., Hasan, S.S., Moll, I., Carvajal, S., Jiménez, W., Starostecka, M., Billeter, A.T., Müller-Stich, B., Wolff, G., Ekim-Üstünel, B., Herzig, S., Mogler, C., Fischer, A., and Rodriguez-Vita, J. (2023). "Semaphorin 3C exacerbates liver fibrosis." Hepatology.DOI: 10.1101/2021.07.29.454292.

De Silva, D.M., Roy, A., Kato, T., Cecchi, F., Lee, Y.H., Matsumoto, K., and Bottaro, D.P. (2017). "Targeting the hepatocyte growth factor/Met pathway in cancer." Biochem Soc Trans **45**(4): 855-870.DOI: 10.1042/BST20160132.

Del Campo, J.A., Gallego, P., and Grande, L. (2018). "Role of inflammatory response in liver diseases: Therapeutic strategies." World J Hepatol **10**(1): 1-7.DOI: 10.4254/wjh.v10.i1.1.

DeLeve, L.D. (2013). "Liver sinusoidal endothelial cells and liver regeneration." J Clin

Invest **123**(5): 1861-1866.DOI: 10.1172/JCI66025.

Deleve, L.D., Wang, X., and Guo, Y. (2008a). "Sinusoidal endothelial cells prevent rat stellate cell activation and promote reversion to quiescence." Hepatology **48**(3): 920-930.DOI: 10.1002/hep.22351.

DeLeve, L.D., Wang, X., Hu, L., McCuskey, M.K., and McCuskey, R.S. (2004). "Rat liver sinusoidal endothelial cell phenotype is maintained by paracrine and autocrine regulation." Am J Physiol Gastrointest Liver Physiol **287**(4): G757-763.DOI: 10.1152/ajpgi.00017.2004.

DeLeve, L.D., Wang, X., Kanel, G.C., Atkinson, R.D., and McCuskey, R.S. (2008b). "Prevention of hepatic fibrosis in a murine model of metabolic syndrome with nonalcoholic steatohepatitis." Am J Pathol **173**(4): 993-1001.DOI: 10.2353/ajpath.2008.070720.

Dewidar, B., Meyer, C., Dooley, S., and Meindl-Beinker, A.N. (2019). "TGF-beta in Hepatic Stellate Cell Activation and Liver Fibrogenesis-Updated 2019." Cells **8**(11).DOI: 10.3390/cells8111419.

Dhanda, S., and Sandhir, R. (2018). "Blood-Brain Barrier Permeability Is Exacerbated in Experimental Model of Hepatic Encephalopathy via MMP-9 Activation and Downregulation of Tight Junction Proteins." Mol Neurobiol **55**(5): 3642-3659.DOI: 10.1007/s12035-017-0521-7.

Dimmeler, S., and Zeiher, A.M. (2000). "Endothelial Cell Apoptosis in Angiogenesis and Vessel Regression." Circ Res **87**(6): 434-439.DOI: 10.1161/01.res.87.6.434.

Ding, B.S., Cao, Z., Lis, R., Nolan, D.J., Guo, P., Simons, M., Penfold, M.E., Shido, K., Rabbany, S.Y., and Rafii, S. (2014). "Divergent angiocrine signals from vascular niche balance liver regeneration and fibrosis." Nature **505**(7481): 97-102.DOI: 10.1038/nature12681.

Dong, S., Chen, Q.-L., Song, Y.-N., Sun, Y., Wei, B., Li, X.-Y., Hu, Y.-Y., Liu, P., and Su, S.-B. (2016). "Mechanisms of CCl4-induced liver fibrosis with combined transcriptomic and proteomic analysis." J Toxicol Sci **41**(4): 561-572.DOI: 10.2131/jts.41.561.

Duan, J.L., Ruan, B., Yan, X.C., Liang, L., Song, P., Yang, Z.Y., Liu, Y., Dou, K.F., Han, H., and Wang, L. (2018). "Endothelial Notch activation reshapes the angiocrine of sinusoidal endothelia to aggravate liver fibrosis and blunt regeneration in mice." Hepatology **68**(2): 677-690.DOI: 10.1002/hep.29834.

Duspara, K., Bojanic, K., Pejic, J.I., Kuna, L., Kolaric, T.O., Nincevic, V., Smolic, R., Vcev, A., Glasnovic, M., Curcic, I.B., and Smolic, M. (2021). "Targeting the Wnt Signaling Pathway in Liver Fibrosis for Drug Options: An Update." J Clin Transl Hepatol **9**(6): 960-971.DOI: 10.14218/JCTH.2021.00065.

Ebrahimi, H., Naderian, M., and Sohrabpour, A.A. (2018). "New Concepts on Reversibility and Targeting of Liver Fibrosis; A Review Article." Middle East J Dig Dis **10**(3): 133-148.DOI: 10.15171/mejdd.2018.103.

Fernández-Llama, P., Turner, R., Dibona, G., and Knepper, M.A. (1999). "Renal expression of aquaporins in liver cirrhosis induced by chronic common bile duct ligation in rats." J Am Soc Nephrol **10**(9): 1950-1957.DOI: 10.1681/ASN.V1091950.

Fernandez, M., Semela, D., Bruix, J., Colle, I., Pinzani, M., and Bosch, J. (2009). "Angiogenesis in liver disease." J Hepatol **50**(3): 604-620.DOI: 10.1016/j.jhep.2008.12.011.

Friedman, S.L. (2003). "Liver fibrosis – from bench to bedside." J Hepatol **38**: 38-53.DOI: 10.1016/s0168-8278(02)00429-4.

Friedman, S.L. (2008). "Hepatic stellate cells: protean, multifunctional, and enigmatic cells of the liver." Physiol Rev **88**(1): 125-172.DOI: 10.1152/physrev.00013.2007.

Fujiyoshi, M., and Ozaki, M. (2011). "Molecular mechanisms of liver regeneration and protection for treatment of liver dysfunction and diseases." Journal of Hepato-Biliary-Pancreatic Sciences **18**(1): 13-22.DOI: 10.1007/s00534-010-0304-2.

Fyffe, C., and Falasca, M. (2013). "3-Phosphoinositide-dependent protein kinase-1 as an emerging target in the management of breast cancer." Cancer Manag Res **5**: 271-280.DOI: 10.2147/CMAR.S35026.

Gagliardi, P.A., Puliafito, A., and Primo, L. (2018). "PDK1: At the crossroad of cancer signaling pathways." Semin Cancer Biol **48**: 27-35.DOI: 10.1016/j.semcancer.2017.04.014.

Gandhi, C.R. (2017). "Hepatic stellate cell activation and pro-fibrogenic signals." J Hepatol **67**(5): 1104-1105.DOI: 10.1016/j.jhep.2017.06.001.

Geerts, A. (2001). "History, heterogeneity, developmental biology, and functions of quiescent hepatic stellate cells." Semin Liver Dis **21**(3): 311-335.DOI: 10.1055/s-2001-17550.

George, J., Wang, S.S., Sevcsik, A.M., Sanicola, M., Cate, R.L., Koteliansky, V.E., and Bissell, D.M. (2000). "Transforming growth factor-beta initiates wound repair in rat liver through induction of the EIIIA-fibronectin splice isoform." Am J Pathol **156**(1): 115-124.DOI: 10.1016/s0002-9440(10)64711-6.

Geraud, C., Evdokimov, K., Straub, B.K., Peitsch, W.K., Demory, A., Dorflinger, Y., Schledzewski, K., Schmieder, A., Schemmer, P., Augustin, H.G., Schirmacher, P., and Goerdt, S. (2012). "Unique cell type-specific junctional complexes in vascular endothelium of human and rat liver sinusoids." PLoS One **7**(4): e34206.DOI: 10.1371/journal.pone.0034206.

Geraud, C., Koch, P.S., Zierow, J., Klapproth, K., Busch, K., Olsavszky, V., Leibing, T., Demory, A., Ulbrich, F., Diett, M., Singh, S., Sticht, C., Breitkopf-Heinlein, K., Richter, K., Karppinen, S.M., Pihlajaniemi, T., Arnold, B., Rodewald, H.R., Augustin, H.G., Schledzewski, K., and Goerdt, S. (2017). "GATA4-dependent organ-specific endothelial differentiation controls liver development and embryonic hematopoiesis." J Clin Invest **127**(3): 1099-1114.DOI: 10.1172/JCI90086.

Grunwald, B., Harant, V., Schaten, S., Fruhschutz, M., Spallek, R., Hochst, B., Stutzer, K., Berchtold, S., Erkan, M., Prokopchuk, O., Martignoni, M., Esposito, I., Heikenwalder, M., Gupta, A., Siveke, J., Saftig, P., Knolle, P., Wohlleber, D., and Kruger, A. (2016). "Pancreatic Premalignant Lesions Secrete Tissue Inhibitor of Metalloproteinases-1, Which Activates Hepatic Stellate Cells Via CD63 Signaling to Create a Premetastatic Niche in the Liver." Gastroenterology **151**(5): 1011-1024 e1017.DOI: 10.1053/j.gastro.2016.07.043.

Grunwald, B., Schoeps, B., and Kruger, A. (2019). "Recognizing the Molecular Multifunctionality and Interactome of TIMP-1." Trends Cell Biol **29**(1): 6-19.DOI: 10.1016/j.tcb.2018.08.006.

Gui, Y., and Dai, C. (2020). "mTOR Signaling in Kidney Diseases." Kidney360 **1**(11): 1319-1327.DOI: 10.34067/KID.0003782020.

Guo, C., Wu, T., Zhu, H., and Gao, L. (2019). "Aquaporin 4 Blockade Attenuates Acute Lung Injury Through Inhibition of Th17 Cell Proliferation in Mice." Inflammation **42**(4): 1401-1412.DOI: 10.1007/s10753-019-01002-4.

Guo, C., Xu, L., He, Q., Liang, T., Duan, X., and Li, R. (2013). "Anti-fibrotic effects of puerarin on CCl4-induced hepatic fibrosis in rats possibly through the regulation of PPAR-gamma expression and inhibition of PI3K/Akt pathway." Food Chem Toxicol **56**: 436-442.DOI: 10.1016/j.fct.2013.02.051.

Hahn, E., Wick, G., Pencev, D., and Timpl, R. (1980). "Distribution of basement membrane proteins in normal and fibrotic human liver. collagen type IV, laminin, and fibronectin." Gut **21**(1): 63-71.DOI: 10.1136/gut.21.1.63.

Han, W., Wang, N., Kong, R., Bao, W., and Lu, J. (2022). "Ligand-activated PPARdelta expression promotes hepatocellular carcinoma progression by regulating the PI3K-AKT signaling pathway." J Transl Med **20**(1): 86.DOI: 10.1186/s12967-022-03288-9.

Han, Y.P., Zhou, L., Wang, J., Xiong, S., Garner, W.L., French, S.W., and Tsukamoto, H. (2004). "Essential role of matrix metalloproteinases in interleukin-1-induced myofibroblastic activation of hepatic stellate cell in collagen." J Biol Chem **279**(6): 4820-4828.DOI: 10.1074/jbc.M310999200.

Hazrati, A., Malekpour, K., Soudi, S., and Hashemi, S.M. (2022). "Mesenchymal Stromal/Stem Cells and Their Extracellular Vesicles Application in Acute and Chronic Inflammatory Liver Diseases: Emphasizing on the Anti-Fibrotic and Immunomodulatory Mechanisms." Front Immunol **13**: 865888.DOI:

10.3389/fimmu.2022.865888.

He, L., Wang, X., Kang, N., Xu, J., Dai, N., Xu, X., and Zhang, H. (2018). "MiR-375 inhibits the hepatocyte growth factor-elicited migration of mesenchymal stem cells by downregulating Akt signaling." Cell Tissue Res **372**(1): 99-114.DOI: 10.1007/s00441-017-2765-y.

Hemmann, S., Graf, J., Roderfeld, M., and Roeb, E. (2007). "Expression of MMPs and TIMPs in liver fibrosis - a systematic review with special emphasis on anti-fibrotic strategies." J Hepatol **46**(5): 955-975.DOI: 10.1016/j.jhep.2007.02.003.

Herbst, H., Frey, A., Heinrichs, O., Milani, S., Bechstein, W.O., Neuhaus, P., and Schuppan, D. (1997). "Heterogeneity of liver cells expressing procollagen types I and IV in vivo." Histochem Cell Biol **107**(5): 399-409.DOI: 10.1007/s004180050126.

Hernandez-Gea, V., and Friedman, S.L. (2011). "Pathogenesis of liver fibrosis." Annu Rev Pathol **6**: 425-456.DOI: 10.1146/annurev-pathol-011110-130246.

Higashi, T., Friedman, S.L., and Hoshida, Y. (2017). "Hepatic stellate cells as key target in liver fibrosis." Adv Drug Deliv Rev **121**: 27-42.DOI: 10.1016/j.addr.2017.05.007.

Hutchins, N.A., Wang, F., Wang, Y., Chung, C.S., and Ayala, A. (2013). "Kupffer cells potentiate liver sinusoidal endothelial cell injury in sepsis by ligating programmed cell death ligand-1." J Leukoc Biol **94**(5): 963-970.DOI: 10.1189/jlb.0113051.

Iredale, J.P. (1997). "Tissue inhibitors of metalloproteinases in liver fibrosis." Int J Biochem Cell Biol **29**(1): 43-54.DOI: 10.1016/s1357-2725(96)00118-5.

Iredale, J.P., Benyon, R.C., Arthur, M.J., Ferris, W.F., Alcolado, R., Winwood, P.J., and N Clark, G.M. (1996). "Tissue inhibitor of metalloproteinase-1 messenger RNA expression is enhanced relative to interstitial collagenase messenger RNA in experimental liver injury and fibrosis." Hepatology **24**(1): 176-184.DOI: 10.1002/hep.510240129.

Jangphattananont, N., Sato, H., Imamura, R., Sakai, K., Terakado, Y., Murakami, K., Barker, N., Oshima, H., Oshima, M., Takagi, J., Kato, Y., Yano, S., and Matsumoto, K. (2019). "Distinct Localization of Mature HGF from its Precursor Form in Developing and Repairing the Stomach." Int J Mol Sci **20**(12).DOI: 10.3390/ijms20122955.

Jarnagin, W.R., Rockey, D.C., Koteliansky, V.E., and S S Wang, D.M.B. (1994). "Expression of variant fibronectins in wound healing: cellular source and biological activity of the EIIIA segment in rat hepatic fibrogenesis." J Cell Biol **127**(6 Pt 2): 2037-2048.DOI: 10.1083/jcb.127.6.2037.

Jia, S., Agarwal, M., Yang, J., Horowitz, J.C., White, E.S., and Kim, K.K. (2018). "Discoidin Domain Receptor 2 Signaling Regulates Fibroblast Apoptosis through PDK1/Akt." Am J Respir Cell Mol Biol **59**(3): 295-305.DOI: 10.1165/rcmb.2017-0419OC.

Jindal, A., Jagdish, R.K., and Kumar, A. (2022). "Hepatic Regeneration in Cirrhosis." J Clin Exp Hepatol **12**(2): 603-616.DOI: 10.1016/j.jceh.2021.08.029.

Kim, S.J., Jung, K.H., Son, M.K., Park, J.H., Yan, H.H., Fang, Z., Kang, Y.W., Han, B., Lim, J.H., and Hong, S.S. (2017). "Tumor vessel normalization by the PI3K inhibitor HS-173 enhances drug delivery." Cancer Lett **403**: 339-353.DOI: 10.1016/j.canlet.2017.06.035.

Koch, P.S., Olsavszky, V., Ulbrich, F., Sticht, C., Demory, A., Leibing, T., Henzler, T., Meyer, M., Zierow, J., Schneider, S., Breitkopf-Heinlein, K., Gaitantzi, H., Spencer-Dene, B., Arnold, B., Klapproth, K., Schledzewski, K., Goerdt, S., and Geraud, C. (2017). "Angiocrine Bmp2 signaling in murine liver controls normal iron homeostasis." Blood **129**(4): 415-419.DOI: 10.1182/blood-2016-07-729822.

Kossakowska, A.E., Edwards, D.R., Lee, S.S., Urbanski, L.S., Stabbler, A.L., Zhang, C.L., Phillips, B.W., Zhang, Y., and Urbanski, S.J. (1998). "Altered balance between matrix metalloproteinases and their inhibitors in experimental biliary fibrosis." Am J Pathol **153**(6): 1895-1902.DOI: 10.1016/S0002-9440(10)65703-3.

Koyama, Y., and Brenner, D.A. (2017). "Liver inflammation and fibrosis." J Clin Invest **127**(1): 55-64.DOI: 10.1172/JCI88881.

Lamalice, L., Le Boeuf, F., and Huot, J. (2007). "Endothelial cell migration during angiogenesis." Circ Res **100**(6): 782-794.DOI: 10.1161/01.RES.0000259593.07661.1e.

Lamszus, K., Joseph, A., Jin, L., Yao, Y., Chowdhury, S., Fuchs, A., Polverini, P.J., Goldberg, I.D., and Rosen, E.M. (1996). "Scatter factor binds to thrombospondin and other extracellular matrix components." Am J Pathol **149**(3): 805-809.

Leibing, T., Geraud, C., Augustin, I., Boutros, M., Augustin, H.G., Okun, J.G., Langhans, C.D., Zierow, J., Wohlfeil, S.A., Olsavszky, V., Schledzewski, K., Goerdt, S., and Koch, P.S. (2018). "Angiocrine Wnt signaling controls liver growth and metabolic maturation in mice." Hepatology **68**(2): 707-722.DOI: 10.1002/hep.29613.

Li, J., Deng, X., Wang, S., Jiang, Q., and Xu, K. (2021). "Resolvin D1 attenuates CCl4 Induced Liver Fibrosis by Inhibiting Autophagy-Mediated HSC activation via AKT/mTOR Pathway." Front Pharmacol **12**: 792414.DOI: 10.3389/fphar.2021.792414.

Liu, L., You, Z., Yu, H., Zhou, L., Zhao, H., Yan, X., Li, D., Wang, B., Zhu, L., Xu, Y., Xia, T., Shi, Y., Huang, C., Hou, W., and Du, Y. (2017). "Mechanotransduction-modulated fibrotic microniches reveal the contribution of angiogenesis in liver fibrosis." Nat Mater **16**(12): 1252-1261.DOI: 10.1038/nmat5024.

Liu, M.L., Mars, W.M., Zarnegar, R., and Michalopoulos, G.K. (1994). "Uptake and distribution of hepatocyte growth factor in normal and regenerating adult rat liver." Am J Pathol **144**(1): 129-140.

Ma, Q., Reiter, R.J., and Chen, Y. (2020). "Role of melatonin in controlling angiogenesis under physiological and pathological conditions." Angiogenesis **23**(2): 91-104.DOI: 10.1007/s10456-019-09689-7.

Maher, J.J., and McGuire, R.F. (1990). "Extracellular matrix gene expression increases preferentially in rat lipocytes and sinusoidal endothelial cells during hepatic fibrosis in vivo." J Clin Invest **86**(5): 1641-1648.DOI: 10.1172/JCI114886.

Mak, K.M., Chen, L.L., and Lee, T.F. (2013). "Codistribution of collagen type IV and laminin in liver fibrosis of elderly cadavers: immunohistochemical marker of perisinusoidal basement membrane formation." Anat Rec (Hoboken) **296**(6): 953-964.DOI: 10.1002/ar.22694.

Makino, Y., Hikita, H., Kodama, T., Shigekawa, M., Yamada, R., Sakamori, R., Eguchi, H., Morii, E., Yokoi, H., Mukoyama, M., Hiroshi, S., Tatsumi, T., and Takehara, T. (2018). "CTGF Mediates Tumor-Stroma Interactions between Hepatoma Cells and Hepatic Stellate Cells to Accelerate HCC Progression." Cancer Res **78**(17): 4902-4914.DOI: 10.1158/0008-5472.CAN-17-3844.

Marrone, G., Russo, L., Rosado, E., Hide, D., Garcia-Cardena, G., Garcia-Pagan, J.C., Bosch, J., and Gracia-Sancho, J. (2013). "The transcription factor KLF2 mediates hepatic endothelial protection and paracrine endothelial-stellate cell deactivation induced by statins." J Hepatol **58**(1): 98-103.DOI: 10.1016/j.jhep.2012.08.026.

Marrone, G., Shah, V.H., and Gracia-Sancho, J. (2016). "Sinusoidal communication in liver fibrosis and regeneration." J Hepatol **65**(3): 608-617.DOI: 10.1016/j.jhep.2016.04.018.

Masumoto, A., and Yamamoto, N. (1991). "Sequestration of a hepatocyte growth factor in extracellular matrix in normal adult rat liver." Biochem Biophys Res Commun **174**(1): 90-95.DOI: 10.1016/0006-291x(91)90489-t.

May, D., Djonov, V., Zamir, G., Bala, M., Safadi, R., Sklair-Levy, M., and Keshet, E. (2011). "A transgenic model for conditional induction and rescue of portal hypertension reveals a role of VEGF-mediated regulation of sinusoidal fenestrations." PLoS One **6**(7): e21478.DOI: 10.1371/journal.pone.0021478.

McConnell, M.J., Kostallari, E., Ibrahim, S.H., and Iwakiri, Y. (2023). "The evolving role of liver sinusoidal endothelial cells in liver health and disease." Hepatology.DOI: 10.1097/HEP.0000000000000207.

Michalopoulos, G.K., and Khan, Z. (2005). "Liver regeneration, growth factors, and amphiregulin." Gastroenterology **128**(2): 503-506.DOI: 10.1053/j.gastro.2004.12.039.

Milani, S., Herbst, H., Schuppan, D., Riecken, E.O., and Stein, H. (1989). "Cellular localization of laminin gene transcripts in normal and fibrotic human liver." Am J Pathol **134**(6): 1175-1182.

Miyazawa, K. (2010). "Hepatocyte growth factor activator (HGFA): a serine protease that links tissue injury to activation of hepatocyte growth factor." FEBS J **277**(10): 2208-2214.DOI: 10.1111/j.1742-4658.2010.07637.x.

Mohammed, F.F., Pennington, C.J., Kassiri, Z., Rubin, J.S., Soloway, P.D., Ruther, U., Edwards, D.R., and Khokha, R. (2005). "Metalloproteinase inhibitor TIMP-1 affects hepatocyte cell cycle via HGF activation in murine liver regeneration." Hepatology **41**(4): 857-867.DOI: 10.1002/hep.20618.

Moon, J.O., Welch, T.P., Gonzalez, F.J., and Copple, B.L. (2009). "Reduced liver fibrosis in hypoxia-inducible factor-1alpha-deficient mice." Am J Physiol Gastrointest Liver Physiol **296**(3): G582-592.DOI: 10.1152/ajpgi.90368.2008.

Myers, P.R., and Tanner, M.A. (1998). "Vascular endothelial cell regulation of extracellular matrix collagen: role of nitric oxide." Arterioscler Thromb Vasc Biol **18**(5): 717-722.DOI: 10.1161/01.atv.18.5.717.

Nakamura, T., and Mizuno, S. (2010). "The discovery of hepatocyte growth factor (HGF) and its significance for cell biology, life sciences and clinical medicine." Proc Jpn Acad Ser B Phys Biol Sci **86**(6): 588-610.DOI: 10.2183/pjab.86.588.

Nakayama, Y., Takahara, T., Miyabayashi, C.R., Itoh, H., Watanabe, A., Sasaki, H., Muragaki, Y., Ooshima, A., and Inoue, K. (1993). "Ultrastructural localization of type IV collagen and laminin in the Disse space of rat liver with carbon tetrachloride induced fibrosis." Liver **11**(5): 260-271.DOI: 10.1111/j.1600-0676.1991.tb00528.x.

Okano, J., Shiota, G., Matsumoto, K., Yasui, S., Kurimasa, A., Hisatome, I., Steinberg, P., and Murawaki, Y. (2003). "Hepatocyte growth factor exerts a proliferative effect on oval cells through the PI3K/AKT signaling pathway." Biochem Biophys Res Commun **309**(2): 298-304.DOI: 10.1016/j.bbrc.2003.04.002.

Olsen, A.L., Bloomer, S.A., Chan, E.P., Gaca, M.D., Georges, P.C., Sackey, B., Uemura, M., Janmey, P.A., and Wells, R.G. (2011). "Hepatic stellate cells require a stiff environment for myofibroblastic differentiation." Am J Physiol Gastrointest Liver Physiol **301**(1): G110-118.DOI: 10.1152/ajpgi.00412.2010.

Overall, C.M., Wrana, J.L., and Sodek, J. (1989). "Independent Regulation of Collagenase, 72-kDa Progelatinase, and Metalloendoproteinase Inhibitor Expression in Human Fibroblasts by Transforming Growth Factor-β." Journal of Biological Chemistry **264**(3): 1860-1869.DOI: 10.1016/s0021-9258(18)94267-5.

Paik, Y.H., Kim, J.K., Lee, J.I., Kang, S.H., Kim, D.Y., An, S.H., Lee, S.J., Lee, D.K., Han, K.H., Chon, C.Y., Lee, S.I., Lee, K.S., and Brenner, D.A. (2009). "Celecoxib induces hepatic stellate cell apoptosis through inhibition of Akt activation and suppresses hepatic fibrosis in rats." Gut **58**(11): 1517-1527.DOI: 10.1136/gut.2008.157420.

Park, H., Lee, S., Shrestha, P., Kim, J., Park, J.A., Ko, Y., Ban, Y.H., Park, D.Y., Ha,

S.J., Koh, G.Y., Hong, V.S., Mochizuki, N., Kim, Y.M., Lee, W., and Kwon, Y.G. (2015). "AMIGO2, a novel membrane anchor of PDK1, controls cell survival and angiogenesis via Akt activation." J Cell Biol **211**(3): 619-637.DOI: 10.1083/jcb.201503113.

Parola, M., and Pinzani, M. (2019). "Liver fibrosis: Pathophysiology, pathogenetic targets and clinical issues." Mol Aspects Med **65**: 37-55.DOI: 10.1016/j.mam.2018.09.002.

Pasarin, M., La Mura, V., Gracia-Sancho, J., Garcia-Caldero, H., Rodriguez-Vilarrupla, A., Garcia-Pagan, J.C., Bosch, J., and Abraldes, J.G. (2012). "Sinusoidal endothelial dysfunction precedes inflammation and fibrosis in a model of NAFLD." PLoS One **7**(4): e32785.DOI: 10.1371/journal.pone.0032785.

Paternostro, C., David, E., Novo, E., and Parola, M. (2010). "Hypoxia, angiogenesis and liver fibrogenesis in the progression of chronic liver diseases." World J Gastroenterol **16**(3): 281-288.DOI: 10.3748/wjg.v16.i3.281.

Phaneuf, D., Moscioni, A.D., LeClair, C., Raper, S.E., and Wilson, J.M. (2004). "Generation of a mouse expressing a conditional knockout of the hepatocyte growth factor gene: demonstration of impaired liver regeneration." DNA Cell Biol **23**(9): 592-603.DOI: 10.1089/dna.2004.23.592.

Poisson, J., Lemoinne, S., Boulanger, C., Durand, F., Moreau, R., Valla, D., and Rautou, P.E. (2017). "Liver sinusoidal endothelial cells: Physiology and role in liver diseases." J Hepatol **66**(1): 212-227.DOI: 10.1016/j.jhep.2016.07.009.

Puche, J.E., Saiman, Y., and Friedman, S.L. (2013). "Hepatic stellate cells and liver fibrosis." Compr Physiol **3**(4): 1473-1492.DOI: 10.1002/cphy.c120035.

Rafii, S., Butler, J.M., and Ding, B.S. (2016). "Angiocrine functions of organ-specific endothelial cells." Nature **529**(7586): 316-325.DOI: 10.1038/nature17040.

Rama Rao, K.V., Verkman, A.S., Curtis, K.M., and Norenberg, M.D. (2014). "Aquaporin-4 deletion in mice reduces encephalopathy and brain edema in experimental acute liver failure." Neurobiol Dis **63**: 222-228.DOI: 10.1016/j.nbd.2013.11.018.

Rao, J., Wang, H., Ni, M., Wang, Z., Wang, Z., Wei, S., Liu, M., Wang, P., Qiu, J., Zhang, L., Wu, C., Shen, H., Wang, X., Cheng, F., and Lu, L. (2022). "FSTL1 promotes liver fibrosis by reprogramming macrophage function through modulating the intracellular function of PKM2." Gut.DOI: 10.1136/gutjnl-2021-325150.

Rescan, P.Y., Loréal, O., Hassell, J.R., Yamada, Y., Guillouzo, A., and Clément, B. (1993). "Distribution and origin of the basement membrane component perlecan in rat liver and primary hepatocyte culture." Am J Pathol **142**(1): 199-208.

Robert, S., Gicquel, T., Victoni, T., Valenca, S., Barreto, E., Bailly-Maitre, B., Boichot, E., and Lagente, V. (2016). "Involvement of matrix metalloproteinases (MMPs) and

inflammasome pathway in molecular mechanisms of fibrosis." Biosci Rep **36**(4).DOI: 10.1042/BSR20160107.

Roeb, E. (2018). "Matrix metalloproteinases and liver fibrosis (translational aspects)." Matrix Biol **68-69**: 463-473.DOI: 10.1016/j.matbio.2017.12.012.

Roeb, E., Purucke, E., Breuer, B., Nguyen, H., Heinrich, P.C., Rose-John, S., and Matern, S. (1997). "TIMP expression in toxic and cholestatic liver injury in rat." J Hepatol **27**(3): 535-544.DOI: 10.1016/s0168-8278(97)80359-5.

Schrage, A., Loddenkemper, C., Erben, U., Lauer, U., Hausdorf, G., Jungblut, P.R., Johnson, J., Knolle, P.A., Zeitz, M., Hamann, A., and Klugewitz, K. (2008). "Murine CD146 is widely expressed on endothelial cells and is recognized by the monoclonal antibody ME-9F1." Histochem Cell Biol **129**(4): 441-451.DOI: 10.1007/s00418-008-0379-x.

Schuppan, D., and Afdhal, N.H. (2008). "Liver Cirrhosis." Lancet **371**(9615): 838-851.DOI: 10.1016/S0140-6736(08)60383-9.

Schuppan, D., and Popov, Y. (2002). "Hepatic fibrosis: from bench to bedside." J Gastroenterol Hepatol: S300-305.DOI: 10.1046/j.1440-1746.17.s3.18.x.

Senoo, H., Yoshikawa, K., Morii, M., Miura, M., Imai, K., and Mezaki, Y. (2010). "Hepatic stellate cell (vitamin A-storing cell) and its relative--past, present and future." Cell Biol Int **34**(12): 1247-1272.DOI: 10.1042/CBI20100321.

Seo, K.W., Sohn, S.Y., Bhang, D.H., Nam, M.J., Lee, H.W., and Youn, H.Y. (2014). "Therapeutic effects of hepatocyte growth factor-overexpressing human umbilical cord blood-derived mesenchymal stem cells on liver fibrosis in rats." Cell Biol Int **38**(1): 106-116.DOI: 10.1002/cbin.10186.

Shan, L., Wang, F., Zhai, D., Meng, X., Liu, J., and Lv, X. (2023). "Matrix metalloproteinases induce extracellular matrix degradation through various pathways to alleviate hepatic fibrosis." Biomed Pharmacother **161**: 114472.DOI: 10.1016/j.biopha.2023.114472.

Son, M.K., Ryu, Y.L., Jung, K.H., Lee, H., Lee, H.S., Yan, H.H., Park, H.J., Ryu, J.K., Suh, J.K., Hong, S., and Hong, S.S. (2013). "HS-173, a novel PI3K inhibitor, attenuates the activation of hepatic stellate cells in liver fibrosis." Sci Rep **3**: 3470.DOI: 10.1038/srep03470.

Su, T., Yang, Y., Lai, S., Jeong, J., Jung, Y., McConnell, M., Utsumi, T., and Iwakiri, Y. (2021). "Single-Cell Transcriptomics Reveals Zone-Specific Alterations of Liver Sinusoidal Endothelial Cells in Cirrhosis." Cell Mol Gastroenterol Hepatol **11**(4): 1139-1161.DOI: 10.1016/j.jcmgh.2020.12.007.

Sufletel, R.T., Melincovici, C.S., Gheban, B.A., Toader, Z., and Mihu, C.M. (2020). "Hepatic stellate cells - from past till present: morphology, human markers, human cell

lines, behavior in normal and liver pathology." Rom J Morphol Embryol **61**(3): 615-642.DOI: 10.47162/RJME.61.3.01.

Svistounov, D., Warren, A., McNerney, G.P., Owen, D.M., Zencak, D., Zykova, S.N., Crane, H., Huser, T., Quinn, R.J., Smedsrod, B., Le Couteur, D.G., and Cogger, V.C. (2012). "The Relationship between fenestrations, sieve plates and rafts in liver sinusoidal endothelial cells." PLoS One **7**(9): e46134.DOI: 10.1371/journal.pone.0046134.

Tatsumi, R. (2010). "Mechano-biology of skeletal muscle hypertrophy and regeneration: possible mechanism of stretch-induced activation of resident myogenic stem cells." Anim Sci J **81**(1): 11-20.DOI: 10.1111/j.1740-0929.2009.00712.x.

Taura, K., De Minicis, S., Seki, E., Hatano, E., Iwaisako, K., Osterreicher, C.H., Kodama, Y., Miura, K., Ikai, I., Uemoto, S., and Brenner, D.A. (2008). "Hepatic stellate cells secrete angiopoietin 1 that induces angiogenesis in liver fibrosis." Gastroenterology **135**(5): 1729-1738.DOI: 10.1053/j.gastro.2008.07.065.

Thabut, D., Routray, C., Lomberk, G., Shergill, U., Glaser, K., Huebert, R., Patel, L., Masyuk, T., Blechacz, B., Vercnocke, A., Ritman, E., Ehman, R., Urrutia, R., and Shah, V. (2011). "Complementary vascular and matrix regulatory pathways underlie the beneficial mechanism of action of sorafenib in liver fibrosis." Hepatology **54**(2): 573-585.DOI: 10.1002/hep.24427.

Toricelli, M., Melo, F.H.M., Hunger, A., Zanatta, D., Strauss, B.E., and Jasiulionis, M.G. (2017). "Timp1 Promotes Cell Survival by Activating the PDK1 Signaling Pathway in Melanoma." Cancers (Basel) **9**(4).DOI: 10.3390/cancers9040037.

Tsuchida, T., and Friedman, S.L. (2017). "Mechanisms of hepatic stellate cell activation." Nat Rev Gastroenterol Hepatol **14**(7): 397-411.DOI: 10.1038/nrgastro.2017.38.

Wang, P.W., Wu, T.H., Lin, T.Y., Chen, M.H., Yeh, C.T., and Pan, T.L. (2019). "Characterization of the Roles of Vimentin in Regulating the Proliferation and Migration of HSCs during Hepatic Fibrogenesis." Cells **8**(10).DOI: 10.3390/cells8101184.

Wang, R., Ding, Q., Yaqoob, U., de Assuncao, T.M., Verma, V.K., Hirsova, P., Cao, S., Mukhopadhyay, D., Huebert, R.C., and Shah, V.H. (2015). "Exosome Adherence and Internalization by Hepatic Stellate Cells Triggers Sphingosine 1-Phosphate-dependent Migration." J Biol Chem **290**(52): 30684-30696.DOI: 10.1074/jbc.M115.671735.

Winkler, M., Staniczek, T., Kurschner, S.W., Schmid, C.D., Schonhaber, H., Cordero, J., Kessler, L., Mathes, A., Sticht, C., Nessling, M., Uvarovskii, A., Anders, S., Zhang, X.J., von Figura, G., Hartmann, D., Mogler, C., Dobreva, G., Schledzewski, K., Geraud, C., Koch, P.S., and Goerdt, S. (2021). "Endothelial GATA4 controls liver fibrosis and regeneration by preventing a pathogenic switch in angiocrine signaling." J Hepatol **74**(2): 380-393.DOI: 10.1016/j.jhep.2020.08.033.

Wisse, E. (1970). "An electron microscopic study of the fenestrated endothelial lining of rat liver sinusoids." J Ultrastruct Res **31**(1): 125-150.DOI: 10.1016/s0022-5320(70)90150-4.

Witek, R.P., Yang, L., Liu, R., Jung, Y., Omenetti, A., Syn, W.K., Choi, S.S., Cheong, Y., Fearing, C.M., Agboola, K.M., Chen, W., and Diehl, A.M. (2009). "Liver cell-derived microparticles activate hedgehog signaling and alter gene expression in hepatic endothelial cells." Gastroenterology **136**(1): 320-330 e322.DOI: 10.1053/j.gastro.2008.09.066.

Xie, G., Choi, S.S., Syn, W.K., Michelotti, G.A., Swiderska, M., Karaca, G., Chan, I.S., Chen, Y., and Diehl, A.M. (2013). "Hedgehog signalling regulates liver sinusoidal endothelial cell capillarisation." Gut **62**(2): 299-309.DOI: 10.1136/gutjnl-2011-301494.

Xie, G., Wang, X., Wang, L., Wang, L., Atkinson, R.D., Kanel, G.C., Gaarde, W.A., and Deleve, L.D. (2012). "Role of differentiation of liver sinusoidal endothelial cells in progression and regression of hepatic fibrosis in rats." Gastroenterology **142**(4): 918-927 e916.DOI: 10.1053/j.gastro.2011.12.017.

Xing, Y., Zhao, T., Gao, X., and Wu, Y. (2016). "Liver X receptor alpha is essential for the capillarization of liver sinusoidal endothelial cells in liver injury." Sci Rep **6**: 21309.DOI: 10.1038/srep21309.

Yan, Z., Qu, K., Zhang, J., Huang, Q., Qu, P., Xu, X., Yuan, P., Huang, X., Shao, Y., Liu, C., Zhang, H., and Xing, J. (2015). "CD147 promotes liver fibrosis progression via VEGF-A/VEGFR2 signalling-mediated cross-talk between hepatocytes and sinusoidal endothelial cells." Clin Sci (Lond) **129**(8): 699-710.DOI: 10.1042/CS20140823.

Yata, Y., Takahara, T., Furui, K., Zhang, L.P., and B Jin, A.W. (1999). "Spatial distribution of tissue inhibitor of metalloproteinase-1 mRNA in chronic liver disease." J Hepatol **30**(3): 425-432.DOI: 10.1016/s0168-8278(99)80101-9.

Yin, C., Evason, K.J., Asahina, K., and Stainier, D.Y. (2013). "Hepatic stellate cells in liver development, regeneration, and cancer." J Clin Invest **123**(5): 1902-1910.DOI: 10.1172/JCI66369.

Yoshiji, H., Kuriyama, S., Miyamoto, Y., Thorgeirsson, U.P., Gomez, D.E., Kawata, M., Yoshii, J., Ikenaka, Y., Noguchi, R., Tsujinoue, H., Nakatani, T., Thorgeirsson, S.S., and Fukui, H. (2000). "Tissue inhibitor of metalloproteinases-1 promotes liver fibrosis development in a transgenic mouse model." Hepatology **32**(6): 1248-1254.DOI: 10.1053/jhep.2000.20521.

Yoshiji, H., Kuriyama, S., Yoshii, J., Ikenaka, Y., Noguchi, R., Nakatani, T., Tsujinoue, H., Yanase, K., Namisaki, T., Imazu, H., and Fukui, H. (2002). "Tissue inhibitor of metalloproteinases-1 attenuates spontaneous liver fibrosis resolution in the transgenic mouse." Hepatology **36**(4 Pt 1): 850-860.DOI: 10.1053/jhep.2002.35625.

Yu, J., Chen, G.G., and Lai, P.B.S. (2021). "Targeting hepatocyte growth factor/c-mesenchymal-epithelial transition factor axis in hepatocellular carcinoma: Rationale and therapeutic strategies." Med Res Rev **41**(1): 507-524.DOI: 10.1002/med.21738.

Zhang, D.W., Zhao, Y.X., Wei, D., Li, Y.L., Zhang, Y., Wu, J., Xu, J., Chen, C., Tang, H., Zhang, W., Gong, L., Han, Y., Chen, Z.N., and Bian, H. (2012). "HAb18G/CD147 promotes activation of hepatic stellate cells and is a target for antibody therapy of liver fibrosis." J Hepatol **57**(6): 1283-1291.DOI: 10.1016/j.jhep.2012.07.042.

Zhang, H., Wang, Y., Lian, L., Zhang, C., and He, Z. (2020). "Glycine-Histidine-Lysine (GHK) Alleviates Astrocytes Injury of Intracerebral Hemorrhage via the Akt/miR-146a-3p/AQP4 Pathway." Front Neurosci **14**: 576389.DOI: 10.3389/fnins.2020.576389.

Zhang, X.J., Olsavszky, V., Yin, Y., Wang, B., Engleitner, T., Ollinger, R., Schledzewski, K., Koch, P.S., Rad, R., Schmid, R.M., Friess, H., Goerdt, S., Huser, N., Geraud, C., von Figura, G., and Hartmann, D. (2020). "Angiocrine Hepatocyte Growth Factor Signaling Controls Physiological Organ and Body Size and Dynamic Hepatocyte Proliferation to Prevent Liver Damage during Regeneration." Am J Pathol **190**(2): 358-371.DOI: 10.1016/j.ajpath.2019.10.009.

Zhang, Y., Hua, L., Lin, C., Yuan, M., Xu, W., Raj, D.A., Venkidasamy, B., Cespedes-Acuna, C.L., Nile, S.H., Yan, G., and Zheng, H. (2022). "Pien-Tze-Huang alleviates CCl4-induced liver fibrosis through the inhibition of HSC autophagy and the TGF-beta1/Smad2 pathway." Front Pharmacol **13**: 937484.DOI: 10.3389/fphar.2022.937484.

Zhangdi, H.J., Su, S.B., Wang, F., Liang, Z.Y., Yan, Y.D., Qin, S.Y., and Jiang, H.X. (2019). "Crosstalk network among multiple inflammatory mediators in liver fibrosis." World J Gastroenterol **25**(33): 4835-4849.DOI: 10.3748/wjg.v25.i33.4835.

Zhao, X., Amevor, F.K., Xue, X., Wang, C., Cui, Z., Dai, S., Peng, C., and Li, Y. (2023). "Remodeling the hepatic fibrotic microenvironment with emerging nanotherapeutics: a comprehensive review." J Nanobiotechnology **21**(1): 121.DOI: 10.1186/s12951-023-01876-5.

Zhao, Y., Ye, W., Wang, Y.D., and Chen, W.D. (2022). "HGF/c-Met: A Key Promoter in Liver Regeneration." Front Pharmacol **13**: 808855.DOI: 10.3389/fphar.2022.808855.

Zoubek, M.E., Trautwein, C., and Strnad, P. (2017). "Reversal of liver fibrosis: From fiction to reality." Best Pract Res Clin Gastroenterol **31**(2): 129-141.DOI: 10.1016/j.bpg.2017.04.005.

8 PUBLICATIONS AND CONGRESS PARTICIPATION

8.1 Publications

Yin, Y.H., Sichler, A, Ecker, J, Laschinger, M, Liebisch, G, Höring, M, Basic, M, Bleich, A, Zhang, X.J., Kübelsbeck, L, Plagge, J, Scherer, E, Wohlleber, D, **Wang**, **J.Y.,** Wang, Y, Steffani, M, Stupakov, P, Gärtner, Y, Lohöfer, F, Mogler, C, Friess, H, Hartmann, D, Holzmann, B, Hüser, N, Janssen, K.P. (2023). "Gut microbiota promote liver regeneration through hepatic membrane phospholipid biosynthesis." J Hepatol. 78(4):820-835. DOI: 10.1016/j.jhep.2022.12.028.

Wang, J.Y., Wang, Y., Steffani, M., Stöß, C., Ankerst, D., Friess, H., Hüser, N., Hartmann, D. (2022). "Novel risk classification based on pyroptosis-related genes defines immune microenvironment and pharmaceutical landscape for hepatocellular carcinoma." Cancers.14(2);447. DOI: 10.3390/cancers14020447.

Zhao, Z.C., Zhao, Z.J., **Wang, J.Y.**, Zhang, H., Xi, Z.F., Xia, Q. (2022). "ABCC6 Knockdown Fuels Cell Proliferation by Regulating PPARα in Hepatocellular Carcinoma." Front Oncol.24(12):840287. DOI: 10.3389/fonc.2022.840287.

Wang, Y., **Wang, J.Y.**, Schnieke, A., Fischer, K. (2021). "Advances in single-cell sequencing: insights from organ transplantation." Mil Med Res.8(1):45. DOI: 10.1186/s40779-021-00336-1.

8.2 Scientific presentation and awards

- Poster presentation at 39th Annual Conference German Association for the Study of the Liver (GASL) held in Bochum, Germany from 27 to 28th January 2023.
- Young Investigator bursary of the European Association for the Study of the

Liver (EASL) organised the International Liver Congress 2022 held in London from 22 to 26th June 2022.

- Oral presentation at Vereinigung der Bayerischen Chirurgen e.V. mit Pflegekongress held in Passau from 20 to 22 July 2022.

9 ACKNOWLEDGEMENTS

Time flies. Three years have passed in a blink of an eye, but I still clearly remember the excitement when I was accepted in 2019 as a doctoral student in the lab of Department of Surgery of Klinikum rechts der Isar affiliated to Technical University of Munich by Prof. Dr. Helmut Friess. From the ignorant teenager who just entered the school to the current medical doctor, I realised the preciousness of scientific research. How precious is life. Looking back on the past, I can clearly see that my growth and progress are inseparable from the support of teachers, brothers, and friends and relatives around me.

First, I would like to express my heartfelt thanks to my supervisor, Prof. Norbert Hüser. You have always treated your work with enthusiasm and had a rigorous scientific attitude toward your studies, which will become a benchmark for my future life, and a goal with which I will continue to move forward. In addition, your care and teaching for your students will be an invaluable asset in our medical careers.

Secondly, I would like to express my sincere thanks to Dr. Daniel Hartmann, who not only led and guided us to form rigorous scientific research thinking and scientific research attitude, but also set an example for us in scientific research work, as well as gave me great support and encouragement in life.

I am very grateful to all my colleagues: Bernhard Holzmann, Marcella Steffani, Johanna Ollesky, Melanie Laschinger, Christian Stöß, Gabriela Holzmann, Felicitas Altmayr, Carolin Mogler, Sarah Schulze, Victor Olsavszky, and Cyrill Géraud for always providing impressive care and support in my study and my life.

I would also like to express my special thanks to my colleagues who have been working in the same department and laboratory: Xuejun Zhang, Baocai Wang, Yang Wang,

Yuhan Yin, Hao Ling. Thank you for your company, encouragement, and support along the way. The clinical goal can be persevering and mighty challenging.

In addition, I sincerely thank my parents and family for their support and spiritual encouragement in my life. They are my strong backing, the warmest harbour, and teach me to face every aspect of life with a positive attitude. A setback is the source of motivation that enables me to go all out and work hard.